Title

Active Genetic Neutralizing Elements for Halting or Deleting Gene Drives

Journal

Molecular Cell, 80(2)

ISSN

1097-2765

Authors

Xu, Xiang-Ru Shannon
Bulger, Emily A
Gantz, Valentino M
et al.

Publication Date

2020-10-01

DOI

10.1016/j.molcel.2020.09.003

Peer reviewed

Molecular Cell

Article

Active Genetic Neutralizing Elements for Halting or Deleting Gene Drives

Graphical Abstract

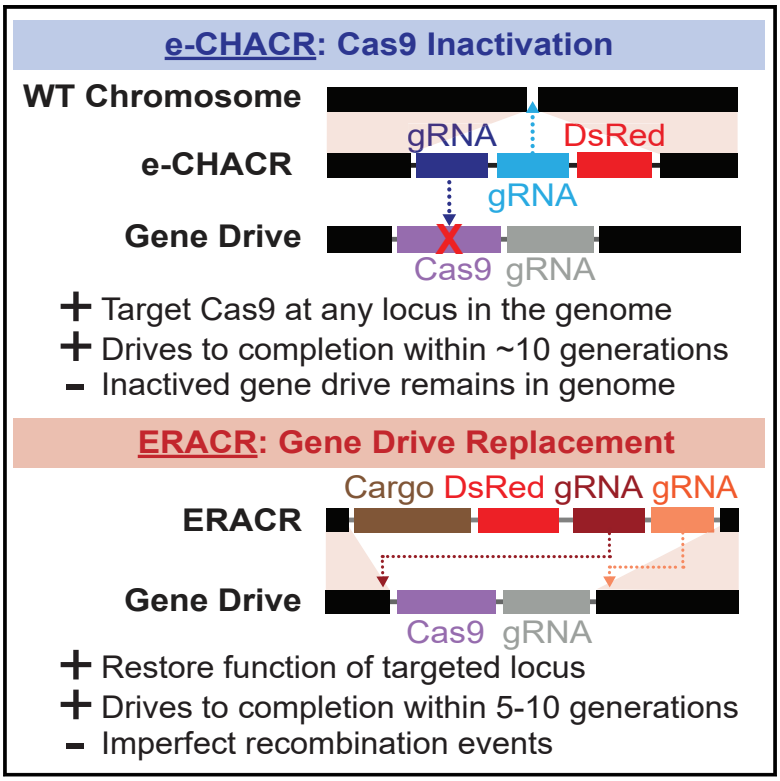

Highlights

- e-CHACRs can efficiently copy and inactivate Cas9 activity (~99%)
- e-CHACRs spread to 100% prevalence in cage trials and eliminate Cas9 activity
- ERACRs often copy but can also damage the target chromosome
- ERACRs can efficiently delete and completely replace a gene drive in population cages

Authors

Xiang-Ru Shannon Xu, Emily A. Bulger, Valentino M. Gantz, ..., Omar S. Akbari, John M. Marshall, Ethan Bier

Correspondence

ebier@ucsd.edu

In Brief

Xu et al. describe two genetic systems for neutralizing an active gene drive that efficiently attenuate drive frequency in both pair crosses and cage-population experiments. These neutralization systems either delete the gene drive from the genome (ERACRs) or inactivate the Cas9 protein (e-CHACRs) to halt the gene drive.

Xu et al., 2020, Molecular Cell *80*, 1–17
October 15, 2020
https://doi.org/10.1016/j.molcel.2020.09.003

CellPress

Molecular Cell

CellPress

Article

Active Genetic Neutralizing Elements for Halting or Deleting Gene Drives

Xiang-Ru Shannon Xu,[1,2,7] Emily A. Bulger,[1,2,3,7] Valentino M. Gantz,[1,2,7] Carissa Klanseck,[1,2] Stephanie R. Heimler,[1,2] Ankush Auradkar,[1,2] Jared B. Bennett,[6] Lauren Ashley Miller,[1,2] Sarah Leahy,[1] Sara Sanz Juste,[1,2] Anna Buchman,[1,2] Omar S. Akbari,[1,2] John M. Marshall,[4,5] and Ethan Bier[1,2,8,*]

[1]Section of Cell and Developmental Biology, University of California, San Diego, La Jolla, CA, USA
[2]Tata Institute for Genetics and Society, University of California, San Diego, La Jolla, CA, USA
[3]Developmental and Stem Cell Biology Graduate Program, University of California, San Francisco, and Gladstone Institutes, San Francisco, CA, USA
[4]Division of Epidemiology and Biostatistics, School of Public Health, University of California, Berkeley, Berkeley, CA, USA
[5]Innovative Genomics Institute, Berkeley, CA, USA
[6]Biophysics Graduate Group, University of California, Berkeley, Berkeley, CA 94720, USA
[7]These authors contributed equally
[8]Lead Contact
*Correspondence: ebier@ucsd.edu
https://doi.org/10.1016/j.molcel.2020.09.003

SUMMARY

CRISPR-Cas9-based gene drive systems possess the inherent capacity to spread progressively throughout target populations. Here we describe two self-copying (or active) guide RNA-only genetic elements, called e-CHACRs and ERACRs. These elements use Cas9 produced in *trans* by a gene drive either to inactivate the *cas9* transgene (e-CHACRs) or to delete and replace the gene drive (ERACRs). e-CHACRs can be inserted at various genomic locations and carry two or more gRNAs, the first copying the e-CHACR and the second mutating and inactivating the *cas9* transgene. Alternatively, ERACRs are inserted at the same genomic location as a gene drive, carrying two gRNAs that cut on either side of the gene drive to excise it. e-CHACRs efficiently inactivate Cas9 and can drive to completion in cage experiments. Similarly, ERACRs, particularly those carrying a recoded cDNA-restoring endogenous gene activity, can drive reliably to fully replace a gene drive. We compare the strengths of these two systems.

INTRODUCTION

Harnessing natural or synthetic gene drives to bias inheritance of beneficial traits in populations was proposed more than 60 years ago (Curtis, 1968), and variations on efficient "low-threshold" systems, such as homing endonucleases (Chevalier and Stoddard, 2001; Macreadie et al., 1985), have been modeled extensively over the past two decades (Burt, 2003; Deredec et al., 2008; Eckhoff et al., 2017). Recently, CRISPR-Cas9 genome editing tools have enabled the development of several highly efficient gene drive (or active genetic) systems in insects (Gantz and Bier, 2015; Gantz et al., 2015; Hammond et al., 2016; Kyrou et al., 2018; Li et al., 2019), yeast (DiCarlo et al., 2015), and bacteria (Valderrama et al., 2019). A mammalian guide RNA (gRNA)-only "split-drive" prototype has also shown significant promise in the mouse (Grunwald et al., 2019).

CRISPR-Cas9-based gene drives propagate by creating double-stranded DNA breaks at the precise site on the homologous chromosome where they are inserted into the genome. In the germline, the homology-directed repair (HDR) pathway copies the gene drive element into the break on the homologous chromosome, resulting in super-Mendelian transmission of that element to progeny. Mathematical modeling predicts that such efficient gene drive systems should spread rapidly throughout a population following logistic growth dynamics, even when released at low seeding levels (Burt, 2003; Eckhoff et al., 2017; Gantz and Bier, 2016).

Discussion in the scientific literature, workshops, and the media has raised several potential concerns, including scenarios in which a low-threshold system spreads beyond its intended zone of application (Adelman et al., 2017; James et al., 2018; National Academies of Sciences, Engineering, and Medicine, 2016; Warmbrod et al., 2020). One mitigation strategy for limiting gene drive systems to a chosen region is to develop neutralizing genetic systems that eliminate or prevent further dissemination of the gene drive.

We previously proposed two designs for self-copying (or "active") neutralizing genetic elements that either inactivate Cas9 carried by a gene drive (e-CHACR [erasing construct hitchhiking on the autocatalytic chain reaction]) or delete and replace the gene drive (ERACR [element reversing the autocatalytic chain reaction) (Gantz and Bier, 2016; Figure 1A). A key design feature of both elements is that they encode gRNAs but not Cas9. e-CHACRs can be inserted into the genome at any desired location and encode two or more gRNAs. One gRNA cuts at the

Please cite this article in press as: Xu et al., Active Genetic Neutralizing Elements for Halting or Deleting Gene Drives, Molecular Cell (2020), https://doi.org/10.1016/j.molcel.2020.09.003

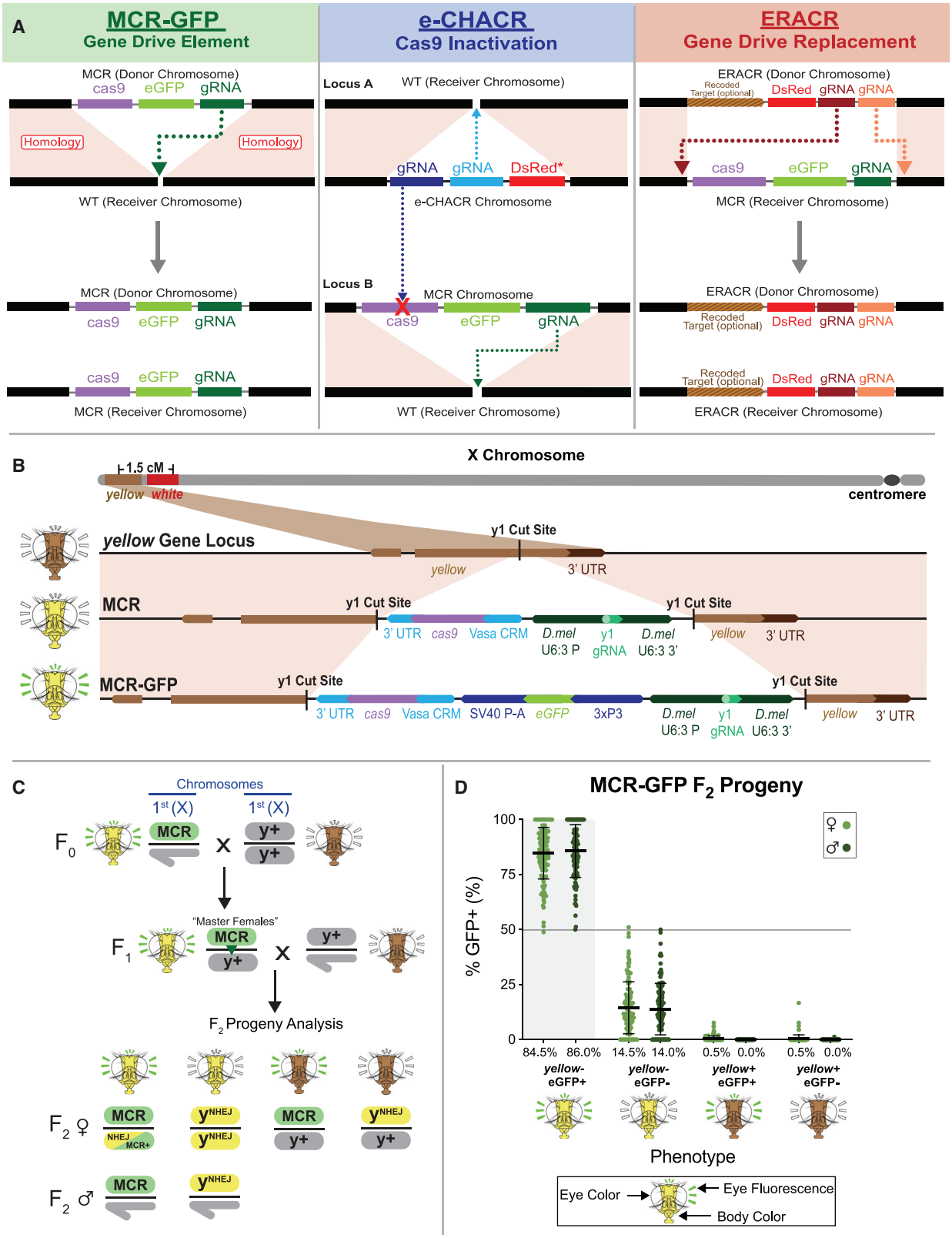

(legend on next page)

Please cite this article in press as: Xu et al., Active Genetic Neutralizing Elements for Halting or Deleting Gene Drives, Molecular Cell (2020), https://doi.org/10.1016/j.molcel.2020.09.003

genomic site of e-CHACR insertion, enabling self-copying in the presence of a *trans*-acting source of Cas9. The additional gRNA(s) target cleavage and inactivation of the *cas9* transgene component of a gene drive element. ERACRs are inserted at the same genomic site as a gene drive and encode two gRNAs that combine with Cas9 produced by the drive, to cut on either side of the drive element to delete and replace it.

When seeded into a gene drive population, such gRNA-only neutralizing systems should follow the same logistic growth trajectory as a gene drive released into a native population (Gantz and Bier, 2016). In the absence of a Cas9 source, however, these neutralizing elements are inherited in a standard Mendelian fashion, as when they have either inactivated (e-CHACR) or eliminated (ERACR) a gene drive element.

In this study, we test and analyze the activities of several e-CHACR and ERACR elements in *Drosophila melanogaster* (*D. mel.*). We find that although the e-CHACRs vary in their copying efficiency, all mutate and inactivate Cas9 efficiently, and the one tested in population cages drives to completion. Similarly, ERACRs often copy and delete a gene drive element as intended but can damage target chromosomes and generate various rare recombinant outcomes. Despite these imperfections, ERACRs, particularly those carrying functional recoded sequences that restore endogenous gene activity, can fully replace a gene drive element in cage experiments. We discuss these results with regard to the potential utility of e-CHACRs and ERACRs to neutralize gene drives.

RESULTS

Active genetic elements such as gene drives and gRNA-only neutralizing elements (Figure 1A) bypass standard rules of inheritance imposed by independent chromosome assortment and linkage of nearby loci. Tracking such fluidly copying elements requires careful genetic bookkeeping by following each genetic element with a different fluorescent transgene and using genetic markers tightly linked to these elements to distinguish donor (chromosome of origin for a given active genetic element) versus receiver (target chromosome to which a drive element copies) chromosome homologs. For example, in this study, we used an eGFP-marked gene drive (mutagenic chain reaction [MCR]-GFP) element inserted in the *yellow* (*y*) locus and DsRed-marked neutralization elements (e-CHACRs and ERACRs). We also marked donor versus receiver X chromosomes either with different alleles of *white* (e.g., *white apricot* [w^a]; phenotype: orange eyes), located 1.5 centimorgans centromere proximal to *y* (Figures 1B and 3A), or a viable allele of the *achaete-scute* locus (ac^4; phenotype: missing innervated thoracic bristles) located immediately nearby (~9 kb centromere proximal to *y*; Figure 2A).

Super-Mendelian Transmission of the MCR-GFP Gene-Drive Element

As a first step in our analysis, we generated an eGFP-marked MCR-GFP gene drive element carrying a *cas9* transgene expressed under control of the *vasa* promoter (*vasa*Cas9) and a gRNA (gRNA-y1) directing its copying at the *y* locus (Gantz and Bier, 2015) using a genetic "tagging" method (STAR Methods; Figure 1B). We assessed the drive performance of the MCR-GFP element in numerous parallel single-pair mating crosses in which so-called F_1 "master females" (females carrying both gRNA and *cas9* transgenes) were crossed to y^+ w^- males (Figure 1C). A substantial fraction (~20%–35%) of crosses resulted in 100% transmission of the MCR-GFP element to all F_2 progeny (Figure 1D). Overall, the MCR-GFP element exhibited an average super-Mendelian transmission rate of ~85%. Similar results were obtained in crosses generated from master females that inherited the drive paternally (Figures 1C and 1D) or maternally (Figures S1A and S1B), albeit with somewhat reduced efficiency in maternal crosses. A noteworthy feature of these experiments, revealed most obviously in histogram summaries of many individual pair matings (Figures S1C–S1D″), was that the frequencies of F_2 progeny inheriting the gene drive element were distributed in a non-Gaussian fashion. Potential explanations for this Poisson-like distribution of gene drive transmission are considered in Data S1. Also, nearly all F_2 progeny displayed a y^- mutant phenotype whether not they carried the MCR-GFP drive, consistent with both zygotically and maternally provided Cas9/gRNA complexes acting on and mutating the wild-type paternal y^+ allele, a phenomenon we and others have previously documented (Champer et al., 2017; Gantz and Bier, 2015; Gantz et al., 2015; Guichard et al., 2019; Hammond et al., 2016; Li et al., 2019; Lin and Potter, 2016).

Experiments with w^a marked receiver chromosomes (Figure S2A) revealed that the two chromosome homologs were inherited following standard Mendelian segregation (Figure S2B). We conclude that the great majority of the super-Mendelian inheritance displayed by the MCR-GFP element in such crosses can be attributed to gene drive copying events rather than to biased transmission of donor versus target receiver chromosomes.

e-CHACRs Efficiently Inactivate Cas9 but Copy with a Range of Frequencies

We inserted e-CHACRs into loci on different chromosomes: the X-linked *white* locus (e-CHACR-wG, eGFP marked; e-CHACR-wR,

Figure 1. Gene-Drive and Neutralizing Drive Elements

(A) Scheme depicting gene drives and neutralizing elements. Left: MCR (mutagenic chain reaction) gene drive element carrying Cas9, an eGFP fluorescent marker, and a gRNA for copying. Center: e-CHACR carrying two or more gRNAs: one gRNA (blue) for copying at its genomic insertion site, a second gRNA (purple) targeting Cas9, and a DsRed (* or eGFP) fluorescent eye marker. e-CHACRs are typically inserted at a different chromosomal site (locus A) than the gene drive (locus B). Right: ERACR carrying gRNAs that target sequences flanking the MCR-GFP element and a DsRed marker.

(B) Two MCR elements inserted at the same site in the *y* locus: (1) MCR lacking a fluorescent marker (third row) and (2) MCR-GFP, an eGFP-marked version (bottom row) carrying the same core components (vasa-Cas9 and gRNA-y1).

(C) Cross scheme for generating MCR-GFP F_1 "master females" and their F_2 progeny. Phenotypes of F_0, F_1, and F_2 progeny are depicted schematically.

(D) Percentage of GFP^+ F_2 progeny (carrying MCR-GFP element) recovered per cross. Fly heads depict eye phenotypes determined by the *white* (*w*) locus: wild-type = w^+ (red eyes), recessive w^- (white eyes), eye fluorescence markers (GFP = radiating green lines), and body color (y^+ = brown, y^- = yellow). Error bars indicate standard deviation; asterisks indicate p values: *$p < 0.05$; **$p < 0.01$; ***$p < 0.001$; and ****$p < 0.0001$.

Please cite this article in press as: Xu et al., Active Genetic Neutralizing Elements for Halting or Deleting Gene Drives, Molecular Cell (2020), https://doi.org/10.1016/j.molcel.2020.09.003

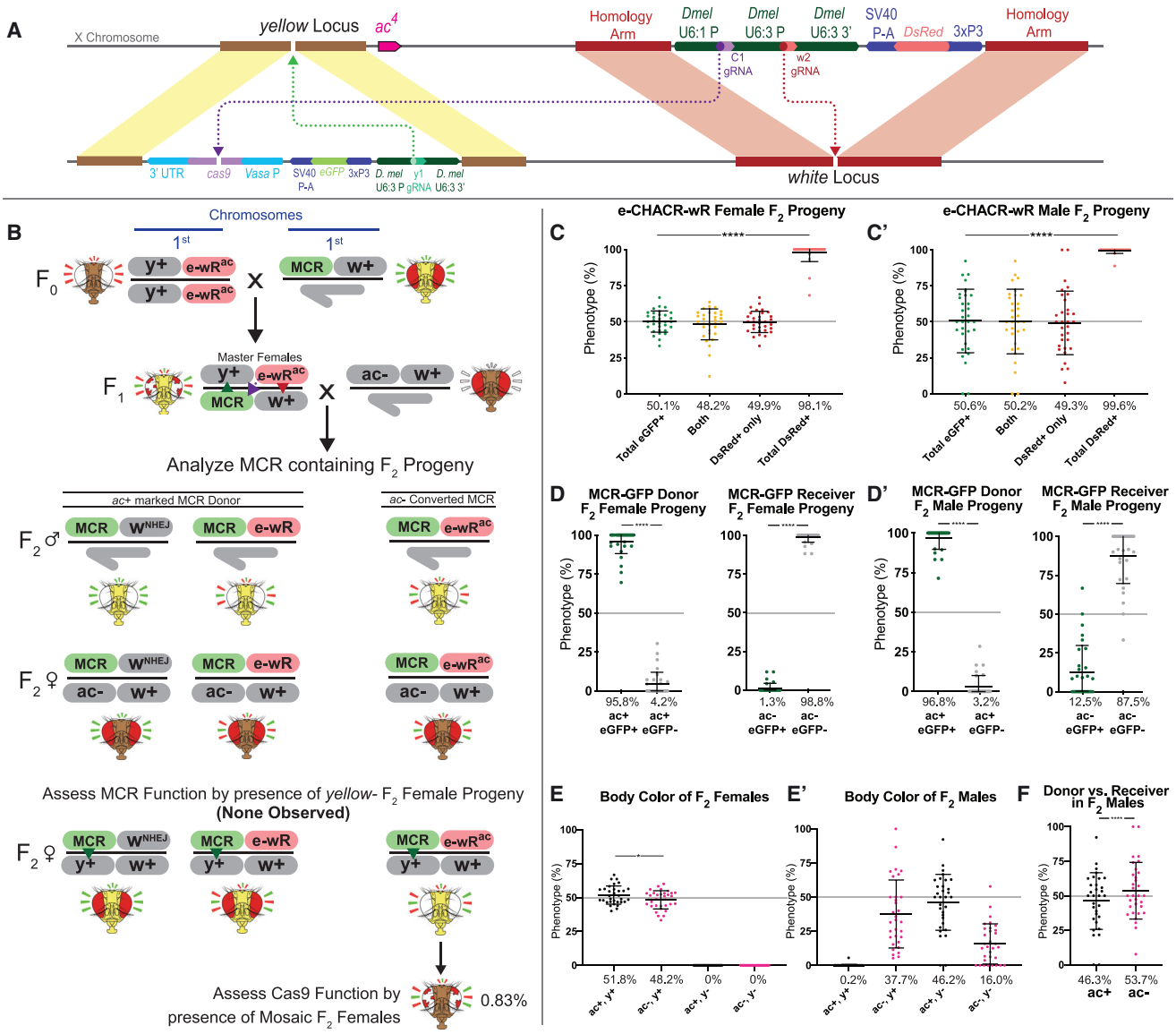

Figure 2. e-CHACR-wR versus the MCR-GFP Element

(A) Schematic of DsRed$^+$ e-CHACR-wR element linked to the y^+ ac^4 allele (e-wR^{ac}) and the y^- ac^+ marked MCR-GFP allele.

(B) Crossing scheme for testing the e-CHACR-wR (e-wR) against the MCR-GFP element. e-CHACR-wR females were mated to MCR-GFP males to generate F_1 master females that were then pair-mated to ac^4 (ac^-) males. F_2 progeny were screened and analyzed for MCR-GFP presence and presence (DsRed$^+$) or absence (w^{NHEJ}) of e-CHACR-wR on ac^+ or ac^4 marked chromosomes.

(C and C′) Percentage of fluorescence phenotypes in total female (C) or male (C′) F_2 progeny per cross.

(D and D′) Prevalence of GFP$^+$ and GFP$^-$ alleles in MCR-GFP donor (left) and receiver (right) F_2 (D) females or (D′) males.

(E and E′) Prevalence of body color in total F_2 (E) females or (E′) males.

(F) Percentage of MCR-GFP donor (ac^+, black dots) and receiver (ac^-, pink dots) alleles in F_2 males. Error bars indicate standard deviation; asterisks indicate p values: *p < 0.05; **p < 0.01; ***p < 0.001; and ****p < 0.0001.

DsRed marked) and the third chromosome *ebony* (e-CHACR-e) and *knirps* (e-CHACR-k) loci (see Data S1 for further details on e-CHACR analysis). Strains carrying these e-CHACRs were crossed to those harboring a standard "static" (non-copying) *vasa*Cas9 source (Figures S3–S5 and S10) or the active MCR-GFP gene drive inserted at *y* (Figure 2; Figures S7–S9 and S11) to generate F_1-generation master females bearing both elements. The phenotypes of F_2 progeny from many parallel pair-mating crosses between F_1 master females and males of informative genotypes (i.e., $y^{\pm}$, $w^{\pm}$, $ac^{\pm}$) were tabulated, as discussed below. We evaluated two key e-CHACR performance parameters: (1) the efficiency of anti-Cas9 gRNAs (gRNA-C1, carried by the *w* and *kni* e-CHACRs, or gRNA-C3, carried by the *ebony* e-CHACR) in mutating and inactivating Cas9 and (2) the rate of e-CHACR copying to the target receiver chromosome.

Please cite this article in press as: Xu et al., Active Genetic Neutralizing Elements for Halting or Deleting Gene Drives, Molecular Cell (2020), https://doi.org/10.1016/j.molcel.2020.09.003

Cas9 inactivation by e-CHACRs was assessed in several ways. For e-CHACRs inserted at *w* (Figure 2; Figures S3, S4, and S7), we monitored a highly penetrant Cas9-dependent somatic mosaic eye phenotype (eyes consist of red and white sectors). By this mosaic eye metric, we estimate that Cas9 was inactivated in ~99% of F_2 progeny by either gRNA-C1 or gRNA-C3, both of which target sites in the *cas9* transgene encoding catalytically essential amino acids. Furthermore, non-mosaic F_2 progeny carrying e-CHACR-wG and the presumably mutated Cas9 source transmitted the GFP^+ element to F_3 progeny at standard Mendelian ratios (Figure S3E), in contrast to the high super-Mendelian frequencies observed in F_2 progeny (Figures S3C and S3C′). In experiments involving the MCR-GFP drive (Figure 2; Figures S7, S9, and S11), we also assessed the full-body y^- pigmentation phenotype, which, as mentioned above, is fully penetrant in F_2 progeny of master females carrying an active MCR-GFP element. 100% of F_2 progeny had y^+ phenotypes, revealing that Cas9 activity was eliminated by all e-CHACRs. We also sequenced genomic DNA isolated from individual F_2 progeny, confirming that the gRNA target sites had been mutated in all samples analyzed from crosses with e-CHACR-wG (carrying gRNA-C1) and e-CHACR-e (carrying gRNA-C3) (Figure S6).

We observed a range of e-CHACR transmission frequencies. Copying was highly efficient (95%–99% transmission to F_2 progeny) for both GFP and DsRed-marked e-CHACRs inserted at *w* (e-CHACR-wG and e-CHACR-wR, respectively) (Figure 2; Figures S3–S5). e-CHACR-k, inserted in the *knirps* (*kni*) locus, exhibited intermediate levels of copying (87%–90% transmission; Figure S11), while e-CHACR-e, inserted at *ebony* (*e*), was transmitted at Mendelian frequencies (Figure S9). The absence of drive for e-CHACR-e was puzzling, as previous experiments with other split-drive elements indicated that the same gRNA-e1 carried by e-CHACR-e sustained modest super-Mendelian copying (López Del Amo et al., 2019). We speculated that efficient mutagenesis of the *cas9* transgene by gRNA-C3 might prevent e-CHACR-e from copying. Indeed, a cleavage-resistant form of the *cas9* transgene (*cas9**) that could not be targeted by gRNA-C3 sustained modest copying of e-CHACR-e (~60% transmission) (Figure S10), similar to that previously reported for the split system driven by the same gRNA-e1 (López Del Amo et al., 2019). We conclude that all three e-CHACRs are highly efficient at eliminating Cas9 activity with either of two Cas9 targeting gRNAs and that their differing transmission most likely reflects the relative activities of the gRNAs that sustain their copying (see Data S1 and Discussion for further analysis).

e-CHACRs Efficiently Inactivate the MCR-GFP Drive

We tested the ability of the three different e-CHACRs to inactivate the MCR-GFP full-drive element, and all functioned efficiently to mutate Cas9, as judged by the virtual absence of F_2 individuals displaying mosaic eye (>99%) or full-body y^- (100%) phenotypes (Figures 2E and 2E′; Figures S9E, S9E′, S11E, and S11E′). All three e-CHACRs also markedly reduced the frequency of MCR-GFP copying, albeit to varying extents. e-CHACR-wR reduced MCR-GFP copying by 5- to 10-fold (i.e., from ~70% [Figure 1D] to 7%–13% [Figures 2D and 2D′]; Figures S7D and S7D′), e-CHACR-e by ~5-fold (Figures S9D and S9D′), and e-CHACR-k by ~2-fold (Figures S11D and S11D′). We conclude that e-CHACRs efficiently inactivate Cas9, copy themselves in the presence of a full-drive element or static sources of Cas9, and significantly reduce copying of the MCR-GFP gene drive element (see Discussion). These various reinforcing activities likely contribute to the efficient performance of e-CHACR-wR in population cage experiments described below.

e-CHACRs Can Preferentially Bias Inheritance of Donor Chromosomes

Visible markers (e.g., w^a, ac^4) closely linked to the e-CHACR and MCR-GFP elements permitted us to determine whether the donor and receiver chromosome homologs segregated in a biased fashion. We observed two types of significant bias in chromosomal inheritance. First, when the X-linked e-CHACR-wG targets a static Cas9 source inserted at the closely linked *y* locus, we observed a nearly 2:1 bias in the inheritance of the donor e-CHACR chromosome over the receiver chromosome in male (Figure S3C′; Figure S4C′) but not female (Figure S3C; Figure S4C) F_2 progeny, which was accompanied by a corresponding excess of females to males (Figures S8B, S8D, and S8F). In contrast, when autosomal e-CHACR-e targeted a nearby Cas9-GFP source at *w*, the single-cut target chromosome was inherited at Mendelian frequencies in F_2 progeny of both sexes (Figure S10A–S10C). Also, e-CHACR-wR driven by an autosomal source of Cas9 did not bias the sex of recovered F_2 progeny (Figure S5). The handicap against receiver chromosomes in the former crosses, however, did not permanently damage target chromosomes, as F_2 females carrying mutated Cas9 chromosomes transmitted them to ~50% of their F_3 progeny (Figure S3E).

The second type of biased chromosome inheritance occurred when any of the three e-CHACRs targeted the MCR-GFP element. In these scenarios, the same locus on both chromosome homologs is targeted for cleavage (the donor MCR-GFP allele with anti-Cas9 gRNAs, and the receiver target allele with gRNA-y1 expressed by the MCR-GFP element). We observed excess transmission of y^+ac^4 receiver chromosomes in F_2 males, but not females (Figure 2F; Figures S7F, S9F, and S11F). We also recovered an unexpected class of GFP^- donor chromosomes (Figures 2D and 2D′; Figures S7D, S7D′, S9D, and S9D′). Of 17 such isogenized GFP^- target chromosomes tested, 10 (59%) carried male-lethal alleles, and all could be rescued by a duplication covering the *y* locus (Figure S12A; Table S1). As analyzed in greater detail in Data S1, we conclude that at least two different types of chromosome bias can be induced by e-CHACR elements: one, seen when cutting chromosomes carrying a static Cas9 source twice, does not irreparably damage the receiver chromosome. The second, associated with e-CHACRs targeting the MCR-GFP drive element, can induce local damage to the donor chromosome resulting in male lethality (or homozygous lethality in females).

ERACR versus MCR-GFP Crossing Schemes

We tested three DsRed-marked ERACR constructs designed to delete and replace the MCR-GFP element inserted at *y* (see Data S2 for in-depth analysis of ERACRs). All three ERACRs carry two gRNAs (gRNA-y2 and gRNA-y3) that direct Cas9 cleavage to either side of the MCR-GFP element (Figure 3A). ERACR-min carries just the aforementioned minimal elements (DsRed and

Please cite this article in press as: Xu et al., Active Genetic Neutralizing Elements for Halting or Deleting Gene Drives, Molecular Cell (2020), https://doi.org/10.1016/j.molcel.2020.09.003

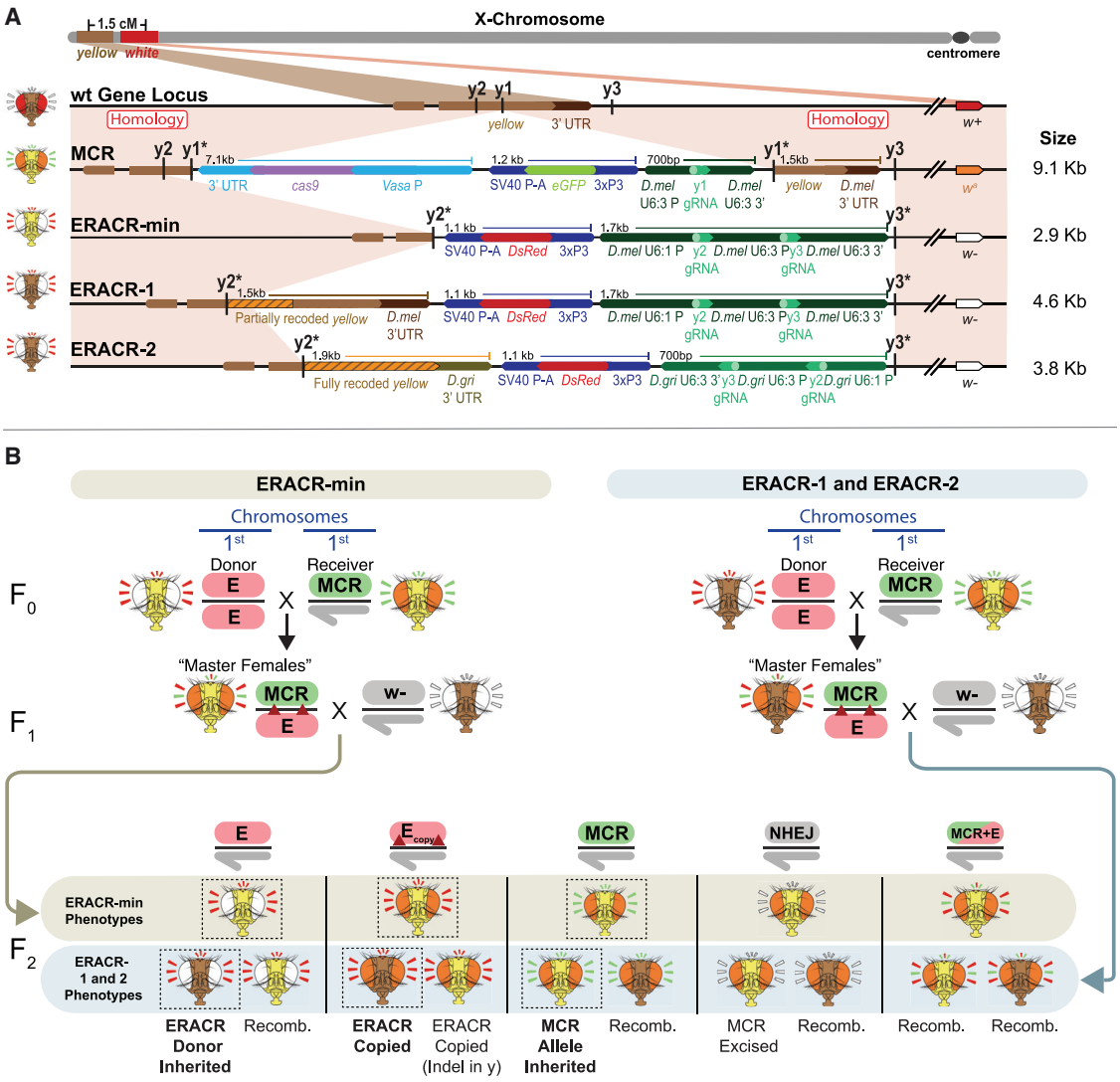

Figure 3. ERACR Construct Designs and Crossing Schemes

(A) Diagrams of MCR-GFP and ERACR elements. Fly heads on the left indicate the phenotype of each strain. Schematic not drawn to scale.

(B) Cross schemes to generate F_1 "master females" with ERACRs in *trans* to the MCR-GFP element and their F_2 progeny. Crossing schemes for y^- ERACR-min (left) and for y^+ ERACR-1 and y^+ ERACR-2 (right). Fly heads depict eye color (wild-type = w^+ [red], w^- [white], or w^a [orange]), eye fluorescence (radial emanating lines of eGFP [green], DsRed [red], both eGFP and DsRed [alternating green and red], or neither fluorescence [white]), and body color: y^+ (brown) or y^- (yellow). Expected F_2 phenotypes are bolded and outlined with dashed black boxes.

two gRNAs), while ERACR-1 and ERACR-2 also carry recoded *y* cDNA coding sequences at their 5′ junction that seamlessly restore function of the *y* locus. ERACR-2 shares fewer homologous sequences with the MCR-GFP element than ERACR-1. *y* cDNA sequences are fully recoded for ERACR-2, whereas only the 5′ junction is recoded in ERACR-1. Also, U6-promoter sequences driving expression of gRNAs carried by ERACR-2 derive from a distantly related Drosophilid (*D. grimshawi*), which have little sequence homology and are oriented in the opposite direction to those carried by the MCR-GFP element to minimize potential spurious recombination events between the two elements.

Fly strains carrying the different DsRed$^+$ ERACR constructs were crossed to a w^a marked MCR-GFP strain (Figure 3B; see also Figure S13 and Data S2 for additional crossing schemes and analysis). F_1 master females carrying the w^a MCR-GFP chromosome and w^- ERACR elements were crossed to w^- males and their F_2 progeny scored for fluorescence, eye color, and whole-body pigmentation phenotypes. This scheme permits w^- ERACR-bearing donor chromosomes to be distinguished from w^a MCR-GFP target chromosomes.

ERACRs Frequently Delete and Often Replace a Gene-Drive Element

Three prominent outcomes were observed among progeny inheriting the w^a receiver chromosome: (1) deletion and replacement of the MCR-GFP element with the ERACR (phenotype:

Please cite this article in press as: Xu et al., Active Genetic Neutralizing Elements for Halting or Deleting Gene Drives, Molecular Cell (2020), https://doi.org/10.1016/j.molcel.2020.09.003

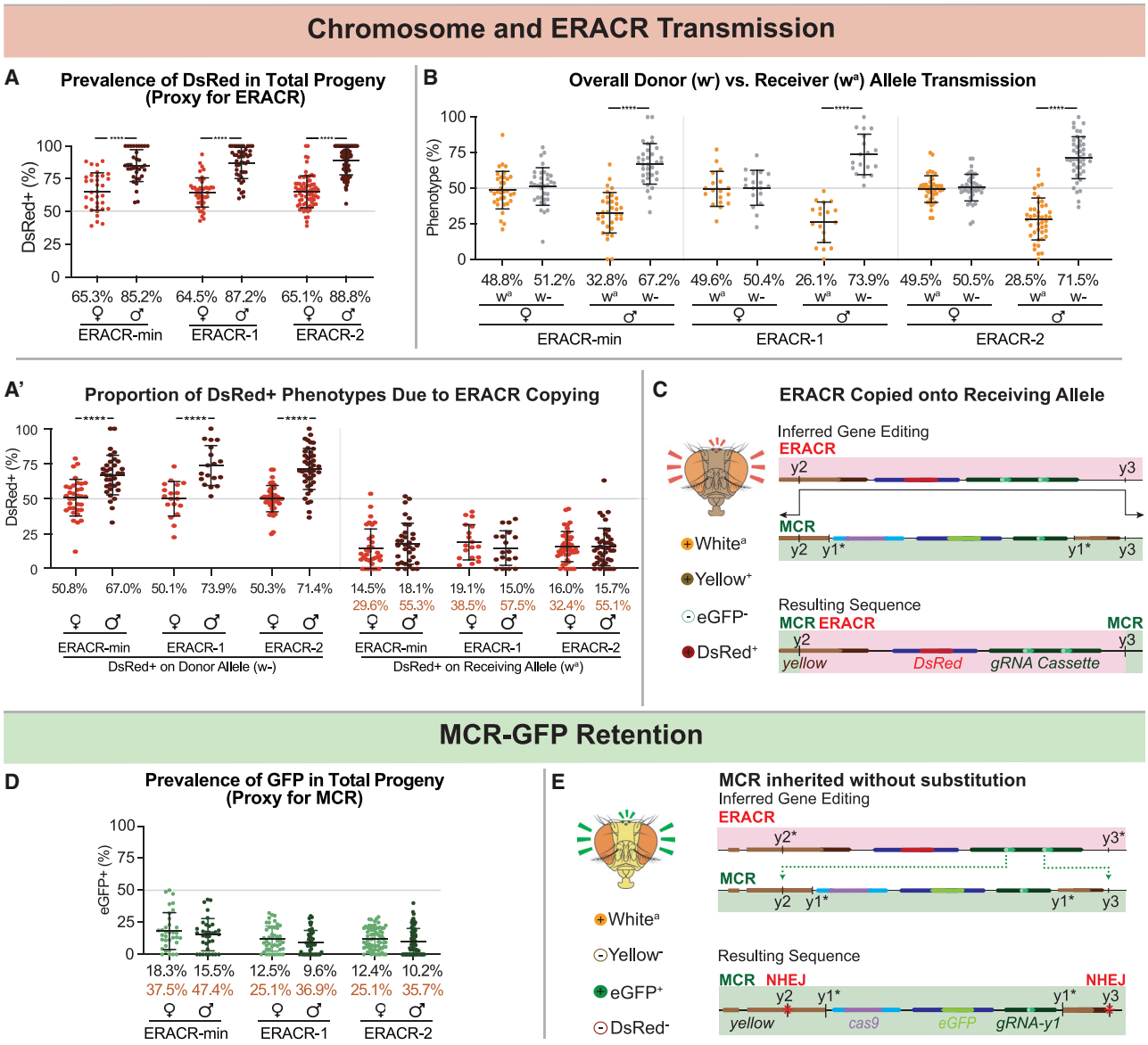

Figure 4. ERACRs Delete and Replace the MCR-GFP Drive

Phenotypic frequencies and deduced gene conversion events in F_2 progeny from crosses depicted in Figure 3A and additional crossing schemes in Figures S13A–S13E. Black type, mean of percentages across all vials; orange type, estimated receiver conversion frequencies (e.g., DsRed w^a males/total w^a males) (see Data S1 for details).

(A) DsRed$^+$ inheritance is a proxy for scoring ERACR prevalence (DsRed$^+$,GFP$^-$ and DsRed$^+$,GFP$^+$ progeny included).

(A′) The subset of data plotted in (A) with traceable donor and receiver chromosomes re-plotted by donor (w$^-$; left graph) versus receiver (w^a; right graph) chromosomes.

(B) Proportion of F_2 males or females inheriting the donor (w^-) versus receiver (w^a) chromosome.

(C and E) Schematics illustrating predicted gene conversion events responsible for specific phenotypes: sequences of relevant junctions shown in (Figure S14).

(D) GFP inheritance is a proxy for MCR-GFP prevalence (DsRed$^+$,GFP$^+$ plus DsRed$^-$,GFP$^+$ F_2 progeny).

(E) MCR-GFP alleles, although intact, have NHEJ-induced indels at the y2 and y3 cut sites. Error bars indicate standard deviation; asterisks indicate p values: *p < 0.05; **p < 0.01; ***p < 0.001; and ****p < 0.0001.

DsRed$^+$,GFP$^-$; Figures 4A–4C); (2) retention of the MCR-GFP element (phenotype: DsRed$^-$,GFP$^+$; Figures 4D and 4E) with nonhomologous end joining (NHEJ)-induced indels at both the gRNA-y2 and gRNA-y3 cut sites (i.e., both ERACR gRNAs direct efficient target cleavage); and (3) deletion of the MCR-GFP element without copying the ERACR (phenotype: DsRed$^-$,GFP$^-$; Figures 5A–5E), a category abundantly observed only in females. Comprehensive analysis of the various ERACR

Please cite this article in press as: Xu et al., Active Genetic Neutralizing Elements for Halting or Deleting Gene Drives, Molecular Cell (2020), https://doi.org/10.1016/j.molcel.2020.09.003

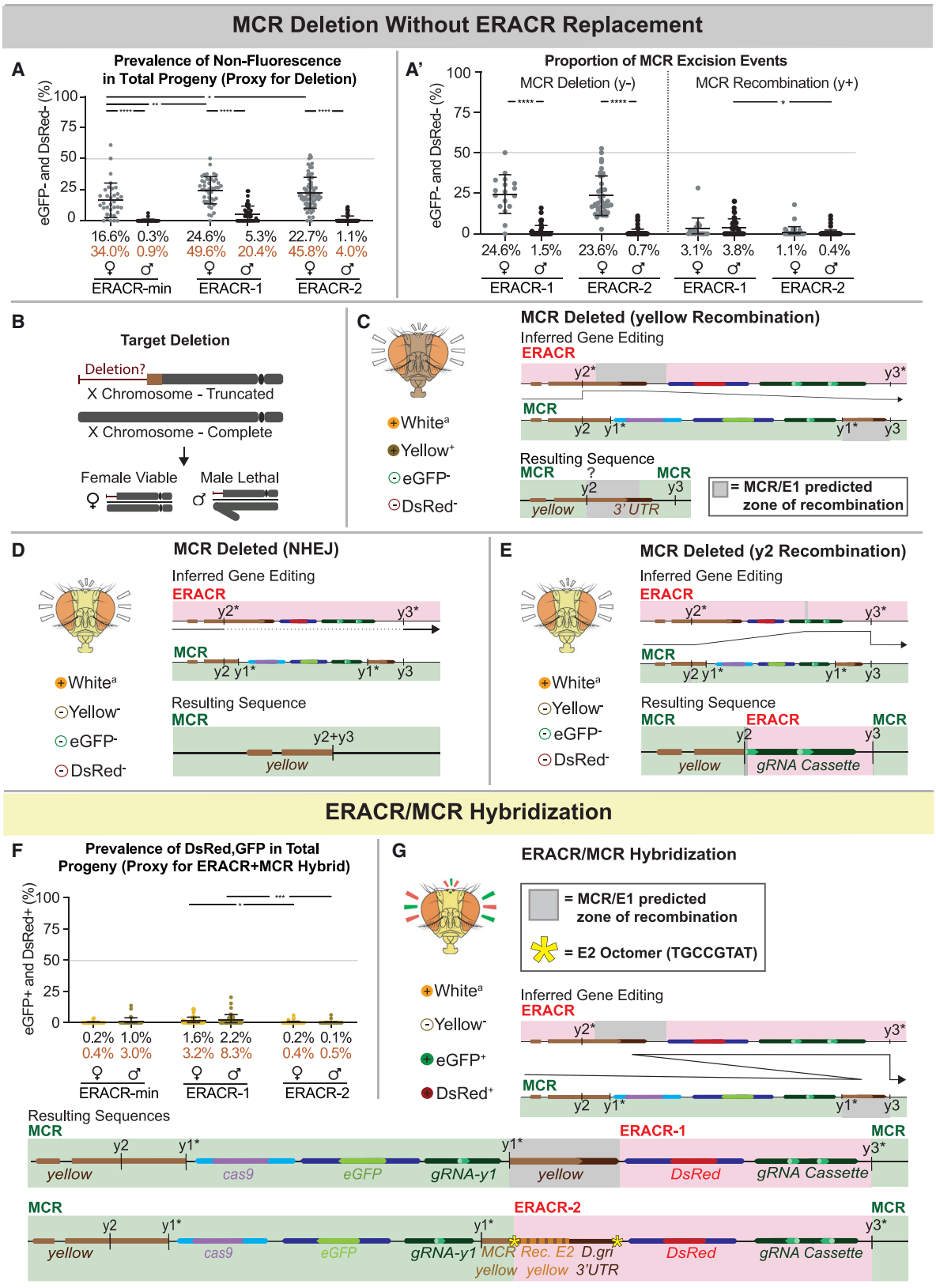

(legend on next page)

Please cite this article in press as: Xu et al., Active Genetic Neutralizing Elements for Halting or Deleting Gene Drives, Molecular Cell (2020), https://doi.org/10.1016/j.molcel.2020.09.003

versus MCR-GFP outcomes is presented in Figure 4, Figure 5, and Figures S14–S17A, and in-depth analysis of these events is presented in Data S2).

Several salient features emerged from these experiments. First, the three ERACRs performed similarly overall (Figures 4 and 5; Figure S15), deleting and replacing the MCR-GFP element (~31%), leaving the MCR-GFP in place (~24%), and, in females, deleting the MCR-GFP without copying (~43%). There were also various rare outcomes (~1%) based on illegitimate recombination events, which differed on the basis of ERACR design (discussed further in Data S2). Second, the DsRed$^-$,GFP$^-$ phenotype was recovered >10-fold more often in females than males (Figures 5A and 5A′). The great majority of such alleles were male lethal, resulting in a 2:1 excess of female over male F_2 progeny (Figure S17A). In all tested cases, lethality of these DsRed$^-$,GFP$^-$ alleles could be rescued by a duplication of the tip of the X chromosome covering the *y* locus (Figure S12B). These findings indicate that ERACRs often damaged the target chromosome, disrupting essential functions in the vicinity of the target locus. Finally, although illegitimate recombinant events were rare, they were recovered (Figures 5C and 5E–5G). A few events lead to the generation of DsRed$^+$,GFP$^+$ mosaic elements (Figures 5F and 5G) that retained some capacity to copy all (Figures S20A–S20C′) or portions (Figures S20D and S20D′) of the elements. Also noteworthy, the frequency of such outlier events was significantly reduced for ERACR-2 relative to ERACR-1 (Figures 5A, 5A′, and 5F; Figures S14 and S15), indicating that elimination of homologous sequences between ERACR and gene drive targets is a favorable design strategy.

One-Sided Homology Mismatch Underlies ERACR-Induced Chromosome Damage

Like e-CHACRs targeting receiver chromosomes for dual cleavage, ERACRs favor inheritance of donor chromosomes, suggesting that ERACR-induced chromosome damage might result from cutting the receiver chromosome twice at neighboring sites. We tested this hypothesis by constructing single-cut versions of ERACR-2, which should not generate damage according to the double-cut model. Single-cut ERACRs carried either only gRNA-y2 (ERACR2-y2, cutting 5′ and centromere distal to the MCR-GFP element), or only gRNA-y3 (ERACR2-y3, cutting 3′ and centromere proximal to the MCR-GFP element) (Figure 6A). We tested these elements for super-Mendelian transmission as well as induction of damage to the target chromosome.

Copying of single-cut ERACRs was assessed by pair-mating them to w^a MCR-GFP individuals according to the scheme depicted in Figure 6B, which is analogous to that used for the double-cut ERACRs (Figure 3B). Analysis of fluorescence associated with w^a receiver chromosomes in F_2 progeny (Figures 6C and 6D) revealed that the frequency of deleting and replacing the MCR-GFP element was significantly reduced for both ERACR2-y2 (average = 4.9%; Figure 6D) and ERACR2-y3 (average = 1.7%; Figure 6D) relative to the dual-cutting ERACR-2 (average = 16%; Figure 4A′, right panels), even when combined.

Crosses of ERACR2-y3 to the MCR-GFP element also reveal whether these single-cut elements might damage the target chromosome. We observed a prominent category (17%) of DsRed$^-$,GFP$^-$ F_2 female progeny that was absent in male siblings (Figure 6C), which is indicative of deleting the MCR-GFP element without copying the ERACR. This rate of DsRed$^-$,GFP$^-$ progeny is similar to that observed for the double-cut ERACR-2 (22.7% in F_2 females versus 1.1% in males; Figure 5A), suggesting that single-cut ERACR2-y3 damages the target chromosome at a frequency comparable with that of the double-cut elements. Although crosses of ERACR2-y2 to the MCR-GFP element did not produce a prominent class of DsRed$^-$,GFP$^-$ F_2 female progeny, we did observe a similar ~10% disparity in the fraction of GFP$^+$ female versus male progeny. This finding could be explained by chromosome damage being induced distal to the gRNA-y2 cut site, leaving the centromere-proximal GFP transgene intact. Both single-cut-ERACRs also lead to an excess of female over male F_2 progeny inheriting the receiver chromosome (Figure S17B), as did all double-cut ERACRs (Figure S17A). These results suggest that both single-cut ERACRs damage the target chromosome at appreciable frequencies and that damage is localized centromere-distal to the gRNA-directed cleavage sites.

We also compared the frequencies with which single- versus double-cut ERACRs copied and induced chromosome damage when confronting a wild-type y^+ allele in a so-called copy-cat configuration with a static source of Cas9 provided in *trans* (Figures S18 and S19). Here, the single-cut ERACR2-y2 (Figure S19B) copied nearly as well as the full double-cut ERACR-2 (Figure S19A), as judged by the proportion of DsRed$^+$,GFP$^+$ progeny (~20%). ERACR2-y3 copied less well, albeit notably better (~6%) than when challenged with the MCR-GFP (~1.5%). Both single- and double-cut ERACRs again induced comparable reductions in transmission of the GFP-marked

Figure 5. Alternative ERACR versus MCR-GFP Outcomes

Partial copying or fusion of sequences on the receiver chromosome.

(A) Non-fluorescent DsRed$^-$,GFP$^-$ F_2 progeny as a proxy for MCR-GFP deletion events (crosses as in Figure 4A).

(A′) Data in (A) re-plotted by inheritance of y^- (lethal deletion) versus y^+ (recombination) alleles. Body color permits inference of the type of excision event that occurred, as depicted in (C)–(E) (data from y^+ F_1 fathers excluded).

(B) Loss of essential sequences distal to the ERACR gRNA cut sites result in male-lethal alleles. Viability of several such alleles can be rescued in males by duplications covering the tip of the X chromosome (Figure S12B).

(C–E) The MCR-GFP element is deleted, but not replaced, by ERACR, producing three distinct observed outcomes. (C) Hypothesized repair mediated by partial pairing of un-recoded *y* sequences carried by ERACR-1 and endogenous *y* sequences 3′ to the MCR-GFP element result in expression of the recoded *y* cassette and a wild-type body color. (D) NHEJ events joining adjacent sequences at the gRNA-y2 and gRNA-y3 cut sites. (E) Likely pairing between 17 bp of the gRNA-y2 genomic target sequences 5′ to the MCR-GFP with correspondingly oriented sequences in the gRNA-y2 transgene carried by either ERACR-min or ERACR-1.

(F) Prevalence of DsRed$^+$,GFP$^+$ F_2 progeny in which MCR-GFP and ERACR sequences are both present on the receiver chromosome.

(G) Two examples of MCR-GFP/ERACR fusion events (see Figure S14). Error bars indicate standard deviation; asterisks indicate p values: *$p < 0.05$; **$p < 0.01$; ***$p < 0.001$; and ****$p < 0.0001$.

Please cite this article in press as: Xu et al., Active Genetic Neutralizing Elements for Halting or Deleting Gene Drives, Molecular Cell (2020), https://doi.org/10.1016/j.molcel.2020.09.003

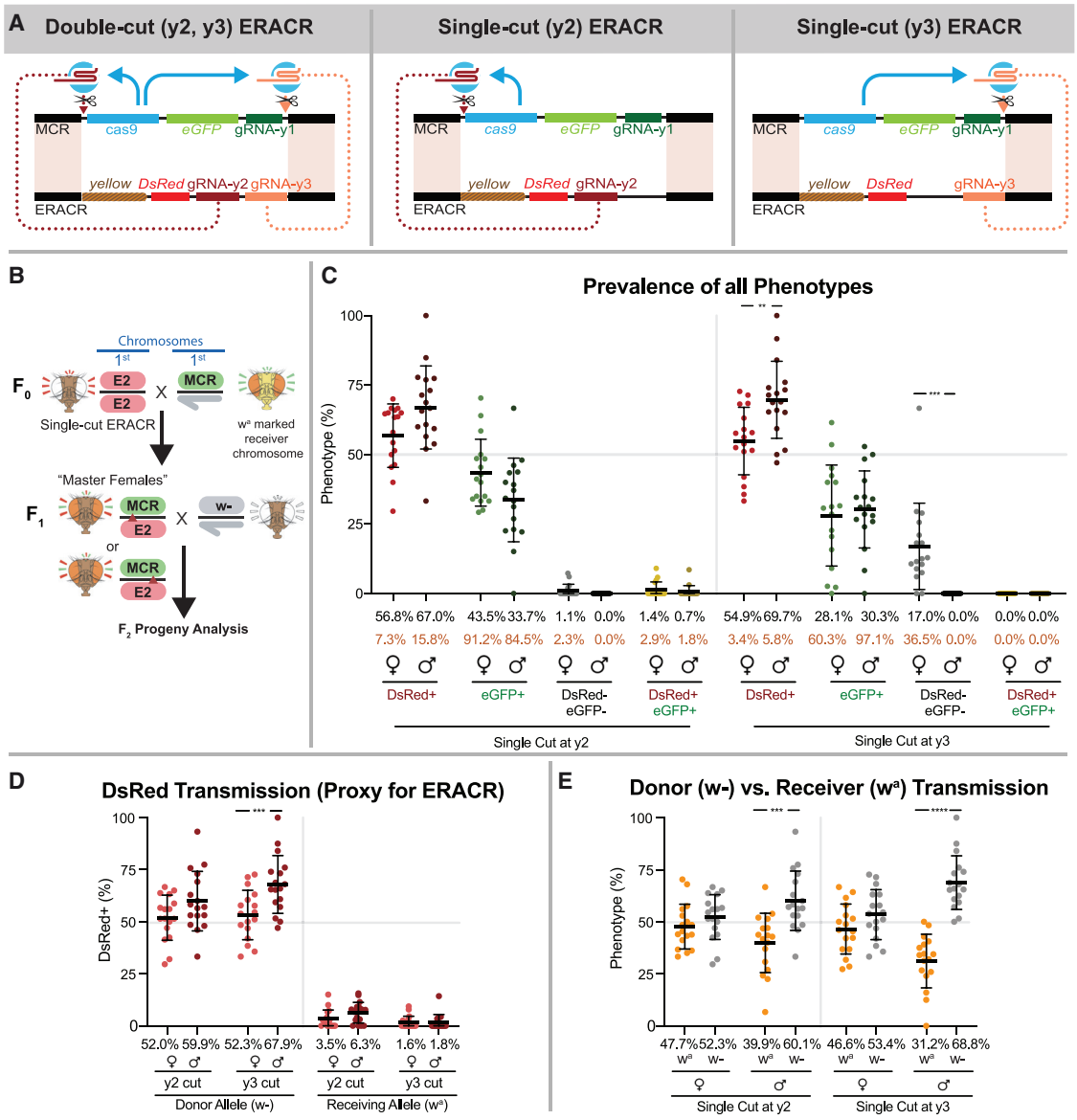

Figure 6. Drive Performance of Single-Cut ERACRs versus MCR-GFP Drive

(A) Schemes illustrating single-cut and double-cut ERACR designs.

(B) Crossing scheme for generating and testing transmission by single-cut w^a ERACR/MCR-GFP F_1 master females.

(C–E) Single-cut versions of ERACR-2 are placed in *trans* to the MCR-GFP element, where the gRNA-y2 and gRNA-y3 are separated by a distance of 11.3 kb (see also Figure S19 for Copy-Cat analysis).

(C) Fluorescent phenotypes for single-cut DsRed$^+$ ERACR2-y2 and ERACR2-y3 and MCR-GFP.

(D) Percent DsRed$^+$ females or males inheriting either the donor (w^-) ERACR-2 single-cut chromosome or the receiver (w^a) chromosome.

(E) Donor versus receiver chromosome transmission for single-cut ERACR2-y2 and ERACR2-y3. Error bars indicate standard deviation; asterisks indicate p values: *p < 0.05; **p < 0.01; ***p < 0.001; and ****p < 0.0001.

target chromosome in F_2 males, but not females, consistent with damage to receiver chromosomes. We conclude that the likely basis for the majority of ERACR-induced chromosomal damage is lack of DNA homology on one side of the ERACR (the side missing the second gRNA), rather than cutting the target chromosome twice. We also note that single-cut ERACRs copy better with less distance between flanking homology sequences (e.g., 2.2 kb in a copy-cat versus 11.3 kb in the MCR-GFP mode).

ERACRs and e-CHACRs Do Not Sustain Shadow Drive

We previously documented a maternal "shadow drive" phenomenon in individuals descended from Cas9-bearing mothers that

Please cite this article in press as: Xu et al., Active Genetic Neutralizing Elements for Halting or Deleting Gene Drives, Molecular Cell (2020), https://doi.org/10.1016/j.molcel.2020.09.003

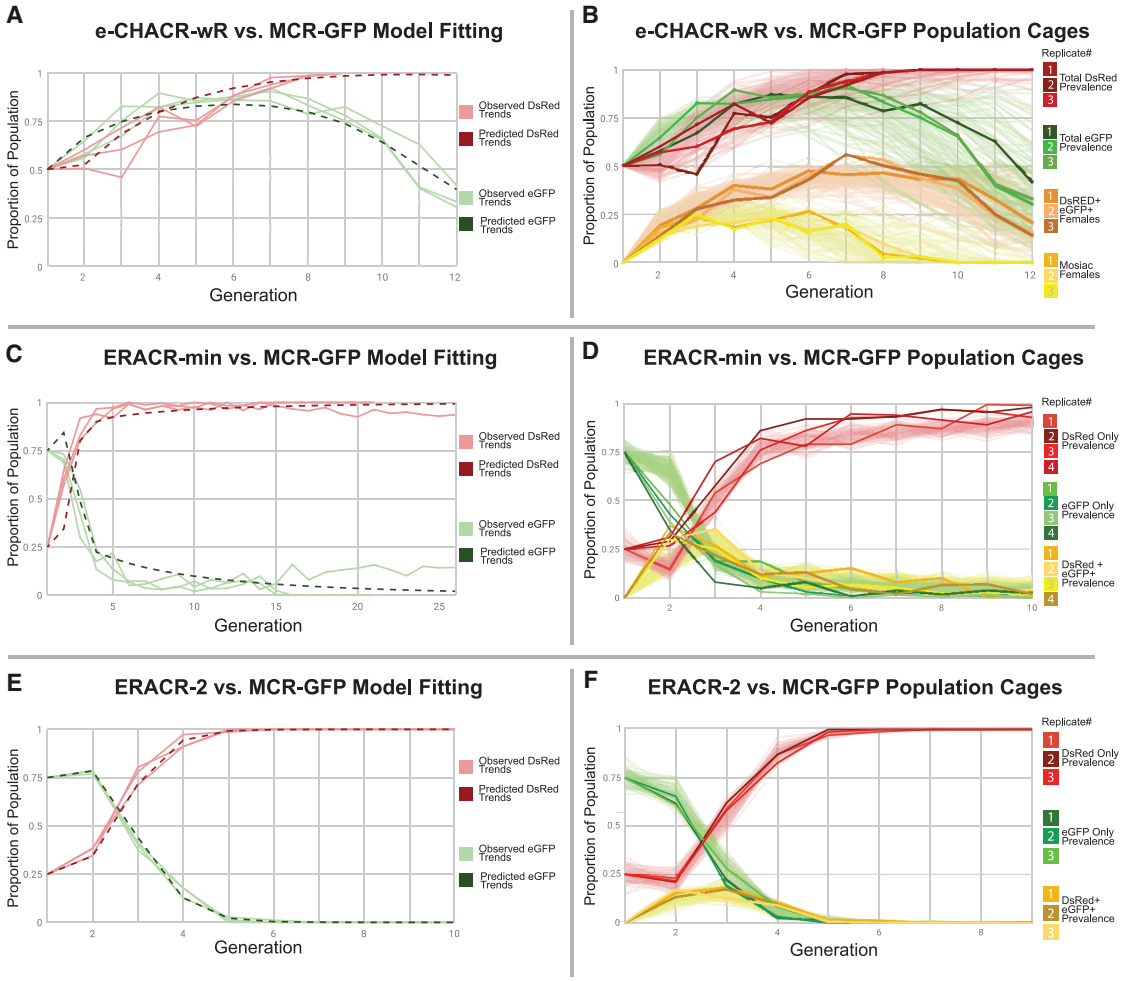

Figure 7. Cage Experiments: MCR-GFP versus e-CHACR-wR and ERACRs

(A–F) Modeling of MCR-GFP versus e-CHACR-wR (A) and ERACR (C and E) dynamics (solid lines; same as B, D, and F) and model fits (dotted lines) plotted for the frequencies of MCR-GFP (green) and e-CHACR-wR or ERACRs (red). (B) Plot of fraction of individuals with different phenotypes over 12 generations. Green, MCR-GFP; red, e-CHACR-wR prevalence in the total population (e.g., both males and females). Orange, females carrying both elements. Yellow, females with mosaic eyes indicative of Cas9 activity. Dark traces represent separate cage replicates, and pale lines denote model simulations (also in D and F). (C and E) Modeling of MCR-GFP versus ERACR dynamics over 26 generations (C) and ERACR-2 (E). (D and F) ERACR-min (D) and ERACR-2 (F) versus MCR-GFP cage experiments. Red, DsRed$^+$ ERACRs; green, MCR-GFP$^+$; yellow, both markers.

inherit a gRNA-based drive element but not the *cas9* transgene (Guichard et al., 2019). As both e-CHACRs and ERACRs eliminate Cas9 activity, we wondered whether this early action might preclude accumulation of sufficient Cas9/gRNA stores to sustain shadow drive in the subsequent generation. We examined the drive potential of e-CHACR or ERACR elements in F_2 progeny of F_1 master females lacking the *cas9* transgene and thus carrying only maternal stores of the endonuclease provided by their F_1 mothers (Figures S21A and S21C). We tested e-CHACR or ERACR transmission to F_3 progeny from such F_2 females and observed Mendelian frequencies of GFP or DsRed transmission, respectively (Figures S21B and S21D–S21F), revealing that neither neutralization element sustained significant shadow drive.

e-CHACR-wR Inactivates the MCR-GFP Gene-Drive in Population Cages

Results from pair-mating crosses revealed that e-CHACR-wR efficiently eliminated Cas9 activity and copied efficiently when combined with either static (Figures S3–S5) or gene drive (Figure 2; Figure S7) borne sources of Cas9. We generated mathematical models on the basis of these single-generation data (Data S1) and fitted parameters on the basis of observed time-series data from the cage trials (Figure S22; Figure 7A, solid lines). These initial values were then used to run simulations, shown as arrays of pale-colored lines, matching the schemes for the different displayed phenotypes (Figure 7B). Simulations with the set of fitted parameters (Data S1, Table S1) were largely consistent with experimental values for the frequencies of

Please cite this article in press as: Xu et al., Active Genetic Neutralizing Elements for Halting or Deleting Gene Drives, Molecular Cell (2020), https://doi.org/10.1016/j.molcel.2020.09.003

different phenotypic classes observed in the pair-mating crosses. We were also able to infer parameters revealing informative deviations from assumptions of random mating between all genotypes. In particular, the modeling indicated a relatively high degree of assortative mating within groups having shared eye pigmentation (i.e., w^+ females preferentially mating with w^+ males over w^- males).

In conjunction with the modeling above, we competed e-CHACR-wR against the MCR-GFP element in population cages. We seeded triplicate cages with equal numbers of homozygous e-CHACR-wR and MCR-GFP individuals. At each generation (n), we scored half of the individuals per cage (approximately 150 random flies) for their fluorescent and $y^{\pm}$ phenotypes, while the other half was used to seed the next generation (n + 1) of cages. In all three cages, e-CHACR (red curves) drove to completion in nine generations (Figures 7A and 7B). In addition, we observed a transient appearance and then disappearance (after eight generations) of a population of DsRed$^+$,GFP$^+$ females that exhibited mosaic eye phenotypes (yellow curves in Figure 7B), which reveals Cas9 activity when the two elements first encounter each other (e.g., as in master females). Outcrosses of sampled DsRed$^+$,GFP$^+$ males and females from generations 9 and 10 revealed that all tested MCR-GFP alleles had lost Cas9 activity (judged by the absence of female progeny with mosaic eyes; Figures S22B and S22B′). In addition, 100% of progeny from crosses of DsRed$^+$,GFP$^+$ females from generations 9 and 10 to wild-type males were DsRed$^+$,GFP$^-$, indicating that the e-CHACR-wR had achieved 100% homozygous introgression (Figures S22C and S22C′). Overall, simulations derived from these assumptions matched well with the observed efficient experimental performance of the e-CHACR (Figure 7B).

Another multi-generational trend was that following an initial expected increase in the MCR-GFP frequency, which peaked at generation 7, prevalence of this element declined precipitously (Figure 7B, green curve). Although a similar trend of initial surge followed by waning was observed in control crosses of the MCR-GFP element to y^- mutants (which harbor an intact gRNA-y1 cleavage site) (Figure S22A), the peak was earlier (generation 5) and the decline more gradual. These later observations suggest that the MCR-GFP element may carry a fitness cost (hence its slow loss in control experiments). The e-CHACR may accelerate clearance of the MCR-GFP element, potentially by inaccurate repair of the targeted *cas9* transgene.

ERACRs Replace the MCR-GFP Gene-Drive in Population Cages

Mathematical modeling on the basis of single-generation pair-mating ERACR data (Figure S15) suggested that these neutralizing elements should also behave as designed to eliminate the gene drive element over multiple generations (Figures 7C and 7E; Figures S23F–S23G′). In these simulations we made the following two simplified assumptions: (1) MCR-GFP elements retained after confrontation with an ERACR are immune to further action by ERACRs (because of generation of cleavage-resistant NHEJ mutations at both cut sites), and (2) double-negative (DsRed$^-$,GFP$^-$) alleles generated by ERACRs deleting, but not replacing, the MCR-GFP element, are fully viable in heterozygous females but lethal in homozygous or hemizygous conditions. In addition, consistent with prior classic studies (Barker, 1962; Bastock, 1956; Diederich, 1941; Merrell, 1949; Sturtevant, 1915), we modeled a range of potential fitness costs for y^- versus ERACR-2 (y^+) males on the basis of y^+ females preferring to mate with y^+ males, as well as an apparent fitness cost associated with the MCR-GFP gene drive. We confirmed a potent assortative mating preference of y^+ females in single-generation control crosses with our own stocks (Figures S23A–S23D) and in competitive multi-generational cage experiments (Figure S23E). Sampling over a broad range of parameters suggested that ERACR-min (y^-) and, particularly, ERACR-2 (y^+) should produce sufficient drive in mixed populations carrying the MCR-GFP and ERACR (but no wild-type alleles) to replace and ultimately eliminate the gene drive over several generations (Figures 7C and 7E).

We conducted three or four separate cage replicates per ERACR composed of 25% homozygous ERACR and 75% homozygous MCR-GFP virgin male and female individuals in each cage. The frequency of the DsRed$^+$ ERACR cassette for the ERACR-min experiment tripled in about four generations and then gradually approached fixation over the next five generations, with a modest degree of variation (~10%–15%) exhibited among the four cages tested (Figure 7D). Reciprocally, the frequency of the MCR-GFP marker decreased until it was nearly eliminated by generation 9. Consistent with random mating among y^- ERACR-min and MCR-GFP individuals, 30%–35% of progeny from the first generation were trans-heterozygotes carrying both fluorescent markers. This double-positive (GFP$^+$,DsRed$^+$) population peaked in generation 3 and then steadily diminished. In contrast, the proportion of DsRed individuals in the ERACR-2 cages (Figure 7F) remained approximately constant for one generation and then increased steeply and in tight synchrony, reaching fixation in five or six generations, with concomitant reduction and then complete elimination of the MCR-GFP element. Notably, ERACR-2 replicates displayed little variation in their drive trajectories. These experimental results match well with simulations (Figures 7D and 7F, pale lines) on the basis of parameters identified by model fitting (Figures 7C and 7E, dotted lines), capturing key features of the overall kinetics and inter-trial variations.

Although there was an excellent overall fit between the observed data and modeling (Figures 7C and 7E; Figure S23F–S23G′), two ERACR-min replicates (1 and 4) pursued moderately different trajectories from the other two (2 and 3), with the latter two matching the predicted modeling (Figures 7C and 7E). As no such events were observed in any of the y^+ ERACR-2 replicates, these outlier trajectories may result from formation of y^- resistance alleles that would have been selected against in the ERACR-2 replicates because of assortative mating but that could persist and potentially spread in the y^- ERACR-min replicates, where they were on even footing. In addition, modeling and cage studies (Figure S22) suggest that a fitness cost is associated with the MCR-GFP element, which might be aggravated by cryptic ERACR-induced damage by gRNA-y2.

We also competed the y^+ ERACR-2 against a y^- NHEJ-induced point allele generated at the gRNA-y1 cleavage site (i.e., the same gRNA driving the MCR-GFP element) in the absence of Cas9 to isolate the effect of assortative mating (Figure S23E). Over about

Please cite this article in press as: Xu et al., Active Genetic Neutralizing Elements for Halting or Deleting Gene Drives, Molecular Cell (2020), https://doi.org/10.1016/j.molcel.2020.09.003

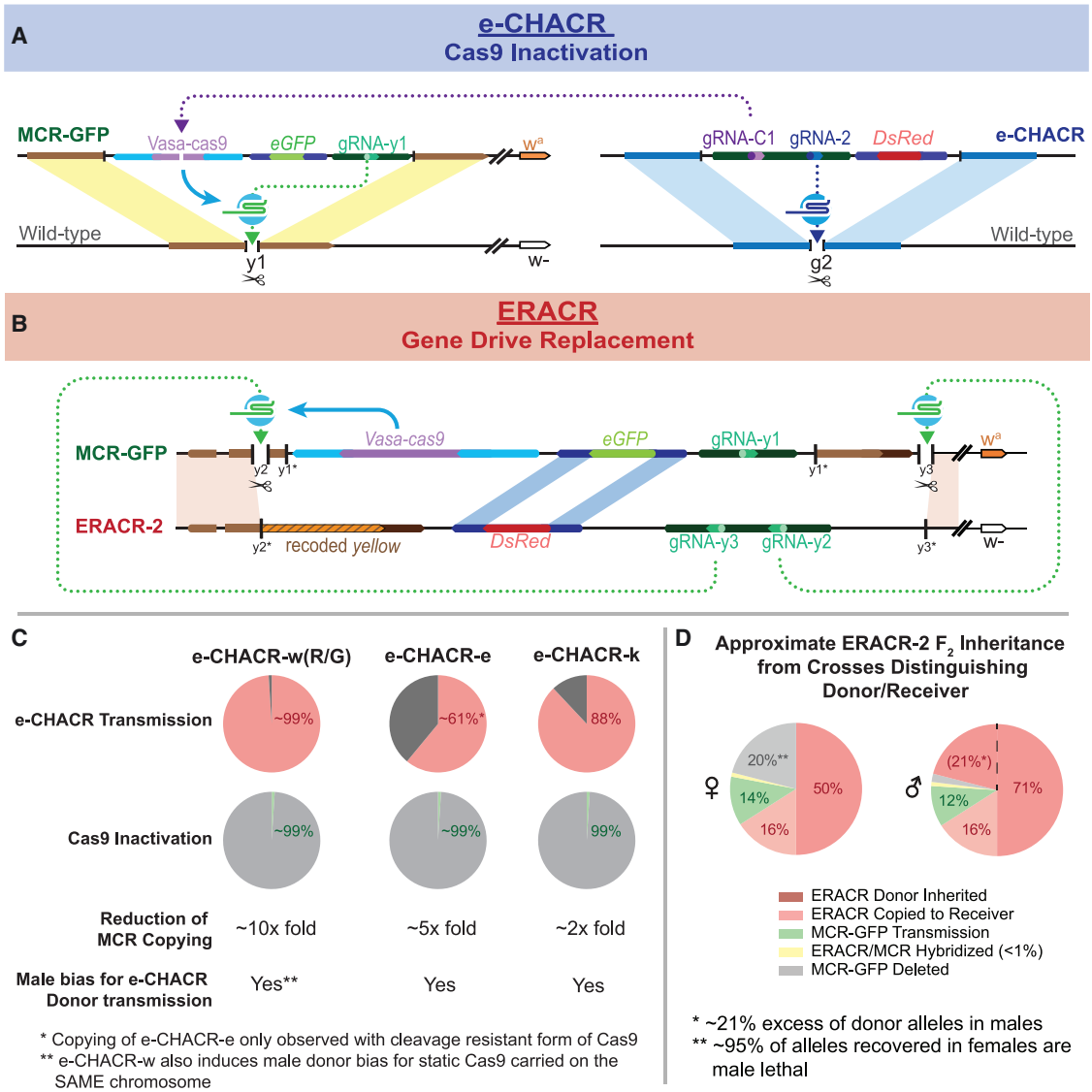

Figure 8. Summary Diagrams

(A) Diagram illustrating the generic action of the e-CHACRs against the MCR-GFP gene drive.

(B) Diagram outlining the structures and homologous sequences serving as sites for potential SDSA-mediated partial copying between ERACR-2 and the MCR-GFP constructs (lightly shaded parallelograms). y1*, y2*, and y3* indicate the loss of the gRNA-y1, gRNA-y2, and gRNA-y3 cut sites accompanying genomic insertion of the MCR-GFP element (gRNA-y1) or ERACRs (gRNA-y2 and gRNA-y3).

(C) Pie charts summarizing key e-CHACR performance parameters.

(D) Pie chart summary of F_2 male and female progeny outcomes derived from F_1 ERACR-2/MCR-GFP master females separated by inferred donor (w^-, red-shaded sectors) versus receiver (w^a: peach, ERACR copied; green, MCR-GFP retention; gray, MCR-GFP deleted) chromosomes.

ten generations, chromosomes carrying the y^+ ERACR-2 successfully overtook the y^- NHEJ population with typical inter-cage variation (Figure S23E). These observations confirm that the y^+ genotype has an appreciable competitive advantage over y^- in a cage setting. Also consistent with y^+ ERACR-2 females mating preferentially with y^+ ERACR-2 males, the frequency of DsRed$^+$,GFP$^+$ (ERACR-2 + MCR-GFP) flies in first-generation progeny (Figure 7F, yellow curves) was considerably lower (15%–20%) than that predicted by random mating (37.5%) or observed for ERACR-min (Figure 7D). We conclude that the modeling predictions conform closely to the experimental outcomes and that ERACRs, particularly those carrying a recoded transgene restoring function of a functionally important gene, have the potential to eliminate and replace a gene drive element even once it has attained fixation in a population.

DISCUSSION

Overall, both e-CHACRs (Figure 8A) and ERACRs (Figure 8B) offer promise for fulfilling their purpose of countering a gene drive

Please cite this article in press as: Xu et al., Active Genetic Neutralizing Elements for Halting or Deleting Gene Drives, Molecular Cell (2020), https://doi.org/10.1016/j.molcel.2020.09.003

system (Figures 8C and 8D), but it is also important to take into account some of their unintended actions.

Drive Performance of Drive and Neutralization Systems

Several factors contribute to levels of drive we observed, which ranged in transmission frequencies from >95% (e-CHACR-wG/R inserted into the *w* locus) to only ~50% Mendelian inheritance (e-CHACR-e, but see below). e-CHACR-k and the MCR-GFP drive element copied at intermediate rates (~85%), which for the MCR-GFP is somewhat lower than estimated in prior experiments in which transmission of an unmarked MCR element was estimated on the basis of full yellow body phenotypes (Gantz and Bier, 2015). As a significant fraction of crosses using the marked MCR-GFP element transmitted it to 100% of progeny, this may also have been the case in those original experiments, which were based on only a small number of crosses. Alternatively, it is possible that we overestimated gene conversion (e.g., the mosaic group might not have inherited the MCR). The size of the drive cassette could also affect copying efficiency, as we have noted higher inheritance rates for a smaller drive element using the same gRNA-y1 (e.g., López Del Amo et al., 2019), which was in the 90% range.

In pair-mating crosses, all three ERACRs deleted the target MCR-GFP gene drive element from 74% of target chromosomes and copied themselves in its place as intended in 31% of those cases. The combined effect of these two outcomes is pronounced super-Mendelian inheritance of ERACR alleles in F_2 males (85%–90%). In females, only copying events contributed to biased inheritance of the ERACR (e.g., ~65%), as male-lethal MCR-deleted chromosomes can survive in the heterozygous state (~20% of total females). In multi-generational contexts, however, damaged alleles carried by females are rapidly purged from the population (see below).

As noted above, e-CHACRs copied at different rates, which most likely reflect relative gRNA efficiencies. Two cases are informative in this regard. First, e-CHACR-e did not copy when combined with Cas9, although in a split-drive configuration, without the Cas9-targeting gRNA, it exhibited modest drive (~60%) (López Del Amo et al., 2019). When combined with a cleavage-resistant Cas9* form, however, e-CHACR-e drove at levels similar to those in the split-drive experiments. We hypothesize that a "weak" gRNA, such as that carried by e-CHACR-e, can fail entirely if the source of Cas9 is eliminated prematurely. Similarly, the intermediate level of MCR-GFP drive (~85%) was reduced 2- to 10-fold when combined with various e-CHACRs, again suggesting that early elimination of Cas9 activity can reduce the performance of suboptimal gRNAs. In contrast, when the e-CHACR-wG/Rs carrying an efficient gRNA were combined with static or MCR-GFP sources of Cas9, they copied at rates equal to those observed in split-drive experiments (López Del Amo et al., 2019). Thus, choosing an efficient gRNA seems to be an important design feature for e-CHACR elements.

ERACRs carry two gRNAs targeting the receiver chromosome at two neighboring sites. The two gRNAs increase the rate of ERACR copying relative to single-cut ERACRs that carry only one or the other gRNA, suggesting some form of synergy even though each gRNA was expected to act independently. This disparity was significantly more pronounced when the two gRNA cut sites were spaced further apart (e.g., when the MCR-GFP element is inserted between them).

Neutralizing Elements Can Bias Chromosomal Inheritance

Marking donor versus receiver chromosomes permitted us to discern three different types of biased inheritance of these chromosome homologs. First, e-CHACRs cutting the same chromosome twice generated a 2:1 bias in favor of transmitting the donor X chromosome in males, but not females. This bias did not lead to any obvious permanent damage, however, because females segregated both donor and receiver chromosomes to their progeny with equal frequency (Figure S3E). Second, e-CHACRs generated a class of donor MCR-GFP alleles lacking the internal GFP marker, more than half of which were male lethal. In this scenario, gRNAs from e-CHACRs (anti-Cas9 gRNAs) and the MCR-GFP element (driving gRNA) target both chromosome homologs in almost exactly same location, a situation most often favoring the receiver allele, which, unlike the *cas9* transgene, is flanked by perfect homology on both sides. Finally, ERACRs with two gRNAs targeting neighboring sites on the same chromosome homolog generated an abundant class of damaged chromosomes. This effect was not the result of dual cutting per se, as single-cut ERACRs generated comparable frequencies of damage. Thus, one-sided homology mismatch rather than dual cutting of the target most likely underlies ERACR-induced chromosome damage.

e-CHACRs and ERACRs Perform Effectively as Designed in Cage Experiments

Despite imperfections revealed in pair matings, e-CHACRs and ERACRs performed largely as intended in multi-generational cage studies. In these experiments, e-CHACR-wR completely eliminated Cas9 activity and drove itself to 100% homozygous introgression in nine or ten generations. Similarly, ERACR-2 entirely replaced the MCR-GFP element over six generations. Several factors contributed to these successful outcomes (Figure 8B): (1) efficient Cas9 mutagenesis by the targeting gRNA, (2) efficient e-CHACR-wR copying, and (3) absence of somatic mosaicism or shadow drive caused by accumulated Cas9/gRNA complexes (this factor, which greatly reduces formation of drive-resistant NHEJ alleles, likewise pertains to ERACR performance). Also, a fitness cost may be associated with the MCR-GFP element, inferred from modeling and competition between the MCR-GFP element and a y^- allele in cages (Figure S22A). In addition, single-generation crosses revealed that e-CHACRs can damage MCR-GFP chromosomes, generating a class of GFP^- male-lethal alleles. These alleles would be invisible in the cage experiments, as they do not survive either in males or homozygous females but would deplete the MCR-GFP allelic pool.

Three notable features distinguished the drive trajectories of y^- ERACR-min and y^+ ERACR-2, all of which derive from their y^- versus y^+ phenotypes. First, ERACR-2 rapidly drove to 100% replacement, while ERACR-min plateaued and then increased more slowly without entirely eliminating the MCR-GFP element. Second, inter-cage variation was much reduced for the ERACR-2 trials than for ERACR-min, for which the observed variation was more typical (~5%–10%). Finally,

ERACR-2 experienced a one-generation lag in producing progeny carrying both the DsRed+ ERACR and MCR-GFP elements (yellow curves in Figure 7D versus Figure 7F).

The significant assortative mating advantage conferred upon y^+ ERACR-2 males relative to y^- MCR-GFP males is well documented (Barker, 1962; Bastock, 1956; Diederich, 1941; Merrell, 1949; Sturtevant, 1915) and was confirmed in our own experiments (Figures S23A–S23E). Indeed, the y^+ ERACR-2 allele overtook a point mutant y^- allele in competitive cage experiments (Figure S23E), albeit more gradually than when driving in a Cas9-dependent fashion against the MCR-GFP element (Figure 7F). The more rapid and complete drive of ERACR-2 compared with ERACR-min can be attributed to dual (Cas9-mediated + assortative mating) versus single (Cas9-mediated) drive mechanisms being operative. Similarly, the initial delay in generating ERACR-2/MCR-GFP heterozygotes is expected if y^+ ERACR-2 females preferentially mated with their own kind. The much reduced inter-cage variation observed for the ERACR-2 trajectories may reflect two independently acting processes: drive produced by Cas9 delivered in *trans* and a selective pressure resulting from assortative mating favoring y^+ males. These dual factors provide fewer opportunities for stochastic variation to accumulate.

Strengths of ERACR and e-CHACR Neutralizing Elements

These studies provide encouraging support for neutralizing a gene drive with e-CHACRs or ERACRs. The major strength of e-CHACRs is that they act generically and can neutralize SpCas9 gene drives inserted at various locations in the genome. e-CHACRs can efficiently inactivate Cas9 and copy themselves (e-CHACR-wG/R elements). The primary advantage of ERACRs is that they can delete and replace the gene drive, thereby eliminating any undesired effect associated with that element. ERACRs perform as intended less often, replacing the gene drive as designed only about a third of the time (Figures 4A and 4B). Nonetheless, ERACRs, particularly ERACR-2 carrying recoded sequences to restore target locus function, performed very effectively in population cages.

In the future, these two neutralizing strategies could be combined to exploit the strengths of each system. These systems also could be implemented with other proposed mitigation measures such as elements carrying anti-Cas9 proteins or inundative releases of strains carrying functional cleavage-resistant alleles of the targeted locus. Such passive elements could spread rapidly if insertion of a gene drive disrupted locus function. Also a CATCHA construct has been described that is inserted at the site of the gene drive (similar to ERACRs) and is designed to copy into the *cas9* transgene (Wu et al., 2016). Although CATCHA elements could target Cas9 sources located elsewhere in the genome, they would not copy in those contexts. Also, because the cassette must be flanked with *cas9* homology arms, it does not readily deliver an in-frame recoded target gene.

Another potential strategy is to incorporate a "weakened" gRNA* targeting the same essential Cas9 amino acid residues as gRNA-C1 or gRNA-C3 into the drive element itself. gRNA*s carrying one or two base pair mismatches to the target sequence should reduce Cas9 cleavage by 1–2 logs. Although not expected to appreciably interfere with the spread of a gene drive carrying such a gRNA*, the *cas9* transgene should be mutated at rates $\sim 10^5$ greater than by spontaneous mutation once the drive attains full introgression into a population, thereby accelerating elimination of Cas9 from the population if it imposed a fitness cost.

Implications for Potential Implementations of Neutralizing Systems

Although e-CHACR and ERACR elements behave largely as expected to curtail the spread of gene drives, they also produce unexpected outcomes (e.g., generation of drive-competent chimeric ERACR/MCR-GFP elements) and can falter in copying (e.g., e-CHACRs with non-optimal gRNAs). Thus, although these experiments provide optimism for strategies to retard wayward gene drive systems if necessary, we agree with the recommendations of the National Academies of Sciences, Engineering, and Medicine (2016) report on gene-drives regarding the cautious use of such neutralization systems. We concur with their appraisal that the decision to go forward with potential releases of gene drive systems should not be predicated on constructing neutralizing elements and that such systems should be developed only for precautionary purposes. If one has concerns about a potential gene drive system somehow going awry, surely such concerns would only be amplified by release of a second element that could generate yet more complex genetic outcomes. Nonetheless, the present in-depth studies provide encouraging support for the use of these types of mitigating strategies should there be an unanticipated need for them.

STAR★METHODS

Detailed methods are provided in the online version of this paper and include the following:

- KEY RESOURCES TABLE
- RESOURCE AVAILABILITY
  - Lead Contact
  - Materials Availability
  - Data and Code Availability
- EXPERIMENTAL MODEL AND SUBJECT DETAILS
  - *Drosophila* rearing and Genetic Experiments
  - Multi-Generational Population cage studies
- METHOD DETAILS
  - Plasmid Construction
  - MCR-GFP construct by "tagging"
  - Microinjection of ERACR and e-CHACR Constructs
  - Recovery of Transformants and Genomic DNA Isolation
  - *Drosophila* PCR and Sequence Analysis
- QUANTIFICATION AND STATISTICAL ANALYSIS
  - Mathematical Modeling
  - Statistical Methods

SUPPLEMENTAL INFORMATION

Supplemental Information can be found online at https://doi.org/10.1016/j.molcel.2020.09.003.

Please cite this article in press as: Xu et al., Active Genetic Neutralizing Elements for Halting or Deleting Gene Drives, Molecular Cell (2020), https://doi.org/10.1016/j.molcel.2020.09.003

ACKNOWLEDGMENTS

We thank Anthony James, Bill McGinnis, Kim Cooper, Sara Werner, members of the Bier laboratory and the anonymous reviewers for comments and suggestions on the manuscript. We thank James Haber for suggesting the idea of testing single-cut versions of the ERACR and Gerard Terradas for helping count crosses during the campus COVID-19 lockdown. These studies were supported by NIH grant R01 GM117321; a Paul G. Allen Frontiers Group Distinguished Investigator Award to E.B.; funding from the Safe Genes program of the Defense Advanced Research Projects Agency (DARPA) (contract HR0011-17-2-0047) to O.S.A., J.M.M., and E.B. (the views, opinions, and/or findings expressed are those of the authors and should not be interpreted as representing the official views or policies of the U.S. government); NIH grant DP5OD023098, which supported V.M.G.; and a gift from the Tata Trusts in India to the Tata Institute for Genetics and Society—University of California, San Diego (TIGS-UCSD).

AUTHOR CONTRIBUTIONS

Conceptualization, E.B. and V.M.G.; Methodology, E.B. and V.M.G.; Investigation, X.-R.S.X., E.A.B., C.K., A.A., S.R.H., L.A.M., S.L., S.S.J., and A.B.; Validation, X.-R.S.X., E.A.B., C.K., A.A., S.R.H., L.A.M., S.L., S.S.J., and A.B.; Formal Analysis, X.-R.S.X., E.A.B., S.R.H., J.B.B., and J.M.M.; Resources, E.B. and V.M.G.; Visualization, X.-R.S.X., E.A.B., S.R.H., Writing – Original Draft, E.B.; Writing – Review & Editing, X.-R.S.X., E.A.B., C.K., S.R.H., J.B.B., J.M.M., and E.B.; Funding Acquisition, E.B. and O.S.A.; Supervision, E.B., X.-R.S.X., and E.A.B.; Project Administration, E.B., X.-R.S.X., E.A.B., and C.K.

DECLARATION OF INTERESTS

E.B., V.M.G., and O.S.A. have equity interest in Synbal Inc. (E.B. and V.M.G.) and Agragene (E.B., V.G., and O.S.A.). These companies may potentially benefit from the research results. E.B. and V.M.G. also serve on the Board of Directors and Scientific Advisory Board for Synbal Inc., and E.B., V.M.G., and O.S.A. serve on the Scientific Advisory Board for Agragene Inc. The terms of these arrangements have been reviewed and approved by the University of California, San Diego, in accordance with its conflict-of-interest policies. All other authors declare no competing interests.

Received: November 23, 2019
Revised: May 3, 2020
Accepted: September 1, 2020
Published: September 18, 2020

SUPPORTING CITATIONS

The following references appear in the Supplemental Information: Bozas et al. (2009); Brunner et al. (2019); Delattre et al. (1995); Do et al. (2014); Drury et al. (2017); Joyce et al. (2012); Lindsley et al. (2016); López Del Amo et al. (2020); Pham et al. (2019); Vella et al. (2017); Wei and Rong, (2007); Xu et al. (2017).

REFERENCES

Adelman, Z., Akbari, O., Bauer, J., Bier, E., Bloss, C., Carter, S.R., Callender, C., Denis, A.C., Cowhey, P., Dass, B., et al. (2017). Rules of the road for insect gene drive research and testing. Nat. Biotechnol. *35*, 716–718.

Barker, J.S. (1962). Studies of selective mating using the yellow mutant of Drosophila melanogaster. Genetics *47*, 623–640.

Bastock, M. (1956). A gene mutation which changes a behaviour pattern. Evolution *10*, 421–439.

Bozas, A., Beumer, K.J., Trautman, J.K., and Carroll, D. (2009). Genetic analysis of zinc-finger nuclease-induced gene targeting in Drosophila. Genetics *182*, 641–651.

Brunner, E., Yagi, R., Debrunner, M., Beck-Schneider, D., Burger, A., Escher, E., Mosimann, C., Hausmann, G., and Basler, K. (2019). CRISPR-induced double-strand breaks trigger recombination between homologous chromosome arms. Life Sci. Alliance *2*, e201800267.

Burt, A. (2003). Site-specific selfish genes as tools for the control and genetic engineering of natural populations. Proc. Biol. Sci. *270*, 921–928.

Champer, J., Reeves, R., Oh, S.Y., Liu, C., Liu, J., Clark, A.G., and Messer, P.W. (2017). Novel CRISPR/Cas9 gene drive constructs reveal insights into mechanisms of resistance allele formation and drive efficiency in genetically diverse populations. PLoS Genet. *13*, e1006796.

Chevalier, B.S., and Stoddard, B.L. (2001). Homing endonucleases: structural and functional insight into the catalysts of intron/intein mobility. Nucleic Acids Res. *29*, 3757–3774.

Curtis, C.F. (1968). Possible use of translocations to fix desirable genes in insect pest populations. Nature *218*, 368–369.

Delattre, M., Anxolabéhère, D., and Coen, D. (1995). Prevalence of localized rearrangements vs. transpositions among events induced by Drosophila P element transposase on a P transgene. Genetics *141*, 1407–1424.

Deredec, A., Burt, A., and Godfray, H.C. (2008). The population genetics of using homing endonuclease genes in vector and pest management. Genetics *179*, 2013–2026.

DiCarlo, J.E., Chavez, A., Dietz, S.L., Esvelt, K.M., and Church, G.M. (2015). Safeguarding CRISPR-Cas9 gene drives in yeast. Nat. Biotechnol. *33*, 1250–1255.

Diederich, G.W. (1941). Non-random mating between yellow-white and wild type *Drosophila melanogaster*. Genetics *26*, 148.

Do, A.T., Brooks, J.T., Le Neveu, M.K., and LaRocque, J.R. (2014). Double-strand break repair assays determine pathway choice and structure of gene conversion events in Drosophila melanogaster. G3 (Bethesda) *4*, 425–432.

Drury, D.W., Dapper, A.L., Siniard, D.J., Zentner, G.E., and Wade, M.J. (2017). CRISPR/Cas9 gene drives in genetically variable and nonrandomly mating wild populations. Sci. Adv. *3*, e1601910.

Eckhoff, P.A., Wenger, E.A., Godfray, H.C., and Burt, A. (2017). Impact of mosquito gene drive on malaria elimination in a computational model with explicit spatial and temporal dynamics. Proc. Natl. Acad. Sci. U S A *114*, E255–E264.

Gantz, V.M., and Bier, E. (2015). Genome editing. The mutagenic chain reaction: a method for converting heterozygous to homozygous mutations. Science *348*, 442–444.

Gantz, V.M., and Bier, E. (2016). The dawn of active genetics. BioEssays *38*, 50–63.

Gantz, V.M., Jasinskiene, N., Tatarenkova, O., Fazekas, A., Macias, V.M., Bier, E., and James, A.A. (2015). Highly efficient Cas9-mediated gene drive for population modification of the malaria vector mosquito Anopheles stephensi. Proc. Natl. Acad. Sci. U S A *112*, E6736–E6743.

Gloor, G.B., et al. (1993). Type I repressors of P element mobility. Genetics *135*, 81–95.

Grunwald, H.A., Gantz, V.M., Poplawski, G., Xu, X.S., Bier, E., and Cooper, K.L. (2019). Super-Mendelian inheritance mediated by CRISPR-Cas9 in the female mouse germline. Nature *566*, 105–109.

Guichard, A., Haque, T., Bobik, M., Xu, X.S., Klanseck, C., Kushwah, R.B.S., Berni, M., Kaduskar, B., Gantz, V.M., and Bier, E. (2019). Efficient allelic-drive in Drosophila. Nat. Commun. *10*, 1640.

Hammond, A., Galizi, R., Kyrou, K., Simoni, A., Siniscalchi, C., Katsanos, D., Gribble, M., Baker, D., Marois, E., Russell, S., et al. (2016). A CRISPR-Cas9 gene drive system targeting female reproduction in the malaria mosquito vector Anopheles gambiae. Nat. Biotechnol. *34*, 78–83.

James, S., Collins, F.H., Welkhoff, P.A., Emerson, C., Godfray, H.C.J., Gottlieb, M., Greenwood, B., Lindsay, S.W., Mbogo, C.M., Okumu, F.O., et al. (2018). Pathway to deployment of gene drive mosquitoes as a potential biocontrol tool for elimination of malaria in sub-Saharan Africa: recommendations of a scientific working group. Am. J. Trop. Med. Hyg. *98* (6_Suppl), 1–49.

Joyce, E.F., Paul, A., Chen, K.E., Tanneti, N., and McKim, K.S. (2012). Multiple barriers to nonhomologous DNA end joining during meiosis in Drosophila. Genetics *191*, 739–746.

Kyrou, K., Hammond, A.M., Galizi, R., Kranjc, N., Burt, A., Beaghton, A.K., Nolan, T., and Crisanti, A. (2018). A CRISPR-Cas9 gene drive targeting doublesex causes complete population suppression in caged Anopheles gambiae mosquitoes. Nat. Biotechnol. *36*, 1062–1066.

Li, M., Yang, T., Kandul, N.P., Bui, M., Gamez, S., Raban, R., Bennett, J., Sánchez, C.H.M., Lanzaro, G.C., Schmidt, H., et al. (2019). Development of a confinable gene-drive system in the human disease vector, *Aedes aegypti*. bioRxiv. https://doi.org/10.1101/645440.

Lin, C.C., and Potter, C.J. (2016). Non-Mendelian dominant maternal effects caused by CRISPR/Cas9 transgenic components in Drosophila melanogaster. G3 (Bethesda) *6*, 3685–3691.

Lindsley, D.L., Hardy, R.W., Ripoll, P., and Lindsley, D. (2016). Gonadal mosaicism induced by chemical treatment of sperm in Drosophila melanogaster. Genetics *202*, 157–174.

López Del Amo, V., Leger, B.S., Cox, K.J., Gill, S., Bishop, A.L., Scanlon, G.D., Walker, J.A., Gantz, V.M., and Choudhary, A. (2019). Small-molecule control of super-Mendelian inheritance in gene drives. bioRxiv. https://doi.org/10.1101/665620.

López Del Amo, V., Bishop, A.L., Sánchez C, H.M., Bennett, J.B., Feng, X., Marshall, J.M., Bier, E., and Gantz, V.M. (2020). A transcomplementing gene drive provides a flexible platform for laboratory investigation and potential field deployment. Nat. Commun. *11*, 352.

Macreadie, I.G., Scott, R.M., Zinn, A.R., and Butow, R.A. (1985). Transposition of an intron in yeast mitochondria requires a protein encoded by that intron. Cell *41*, 395–402.

Merrell, D.J. (1949). Selective mating in Drosophila melanogaster. Genetics *34*, 370–389.

National Academies of Sciences, Engineering, and Medicine (2016). Gene Drives on the Horizon: Advancing Science, Navigating Uncertainty, and Aligning Research with Public Values (The National Academies Press).

Pham, T.B., Phong, C.H., Bennett, J.B., Hwang, K., Jasinskiene, N., Parker, K., Stillinger, D., Marshall, J.M., Carballar-Lejarazú, R., and James, A.A. (2019). Experimental population modification of the malaria vector mosquito, Anopheles stephensi. PLoS Genet. *15*, e1008440.

Sturtevant, A.H. (1915). Experiments on sex recognition and the problem of sexual selection in *Drosophila*. J. Anim. Behav. *5*, 351–366.

Valderrama, J.A., Kulkarni, S.S., Nizet, V., and Bier, E. (2019). A bacterial gene-drive system efficiently edits and inactivates a high copy number antibiotic resistance locus. Nat. Commun. *10*, 5726.

Vella, M.R., Gunning, C.E., Lloyd, A.L., and Gould, F. (2017). Evaluating strategies for reversing CRISPR-Cas9 gene drives. Sci. Rep. *7*, 11038.

Warmbrod, K.L., Kobokovich, K., West, R., Ray, G., Trotochaud, M., and Montague, M. (2020). Gene Drives: Pursuing Opportunities, Minimizing Risk—A Johns Hopkins University Report on Responsible Governance (Johns Hopkins Bloomberg School of Public Health, Center for Health Security).

Wei, D.S., and Rong, Y.S. (2007). A genetic screen for DNA double-strand break repair mutations in Drosophila. Genetics *177*, 63–77.

Wu, B., Luo, L., and Gao, X.J. (2016). Cas9-triggered chain ablation of cas9 as a gene drive brake. Nat. Biotechnol. *34*, 137–138.

Xu, X.S., Gantz, V.M., Siomava, N., and Bier, E. (2017). CRISPR/Cas9 and active genetics-based trans-species replacement of the endogenous *Drosophila kni*-L2 CRM reveals unexpected complexity. eLife *6*, e30281.

Please cite this article in press as: Xu et al., Active Genetic Neutralizing Elements for Halting or Deleting Gene Drives, Molecular Cell (2020), https://doi.org/10.1016/j.molcel.2020.09.003

STAR★METHODS

KEY RESOURCES TABLE

REAGENT or RESOURCE	SOURCE	IDENTIFIER
Bacterial and Virus Strains		
NEB 5-alpha Electrocompetent Competent E. coli	NEB	C2989
Chemicals, Peptides, and Recombinant Proteins		
Q5 Hotstart High-Fidelity 2X Master Mix	NEB	M0494S
Phusion High-Fidelity PCR Master Mix with HF Buffer	Thermo-Fisher	F531S
Platinum SuperFi DNA Polymerase	Thermo-Fisher	12351010
KOD Xtreme Hot Start DNA Polymerase	Millipore	71975
Critical Commercial Assays		
Qiagen Plasmid Midi Kit	Qiagen	12191
QIAquick PCR purification kit	Qiagen	28104
NEBuilder HiFi DNA Assembly Master Mix	NEB	E2621
Deposited Data		
Raw data (counts from fly experiments, construct maps, sequencing chromatograms)	Generated by this study	https://doi.org/10.17632/hjcpd6j8rn.1
Experimental Models: Organisms/Strains		
Oregon-R	Bloomington Drosophila Stock Center	BDSC #5905
W1118	Bloomington Drosophila Stock Center	BDSC #2376
FM7a	Bloomington Drosophila Stock Center	BDSC #785
Basc	Bloomington Drosophila Stock Center	BDSC #806
w[a]	Bloomington Drosophila Stock Center	BDSC #148
ac[4] w[a]	Bloomington Drosophila Stock Center	BDSC #8
w[*]; TM3, Sb[1] Ser[1]/TM6B, Tb[1]	Bloomington Drosophila Stock Center	BDSC#2537
y-; w- (used in MCR cage trial)	Gift from the Gantz Lab	N/A
y-; w- (F5 line used in ERACR cage trial)	Gantz et al., 2015	N/A
Vasa Cas9 in yellow (y1) w[1118A]	Gift from the Gantz Lab	N/A
Vasa Cas9 in yellow (y1) w+	Gift from the Gantz Lab	N/A
Vasa Cas9 in white (w2)	Gift from the Gantz Lab	N/A
w- MCR GFP	This study	N/A
w[a] MCR GFP	This study	N/A
w+ MCR GFP	This study	N/A
e-CHACR-AG; see Table S3	This study	N/A
e-CHACR-AR; see Table S3	This study	N/A
eCHACR-e; see Table S3	This study	N/A
e-CHACR-k; see Table S3	This study	N/A
vCas9-R; see Table S3	This study	N/A
ERACR-min; see Table S3	This study	N/A
ERACR-1; see Table S3	This study	N/A
ERACR-2; see Table S3	This study	N/A
ERACR-2 y2 Single-cut; see Table S3	This study	N/A
ERACR-2 y3 Single-cut; see Table S3	This study	N/A
X-duplication lines; see Table S5	Bloomington Drosophila Stock Center	Various; See Table S5
Oligonucleotides		
Cloning/construct design primers; see Table S2	N/A	N/A
PCR primers; see Table S5	N/A	N/A

(*Continued on next page*)

Please cite this article in press as: Xu et al., Active Genetic Neutralizing Elements for Halting or Deleting Gene Drives, Molecular Cell (2020), https://doi.org/10.1016/j.molcel.2020.09.003

Continued

REAGENT or RESOURCE	SOURCE	IDENTIFIER
Recombinant DNA		
ERACR-min	This study	N/A
ERACR-1	This study	N/A
ERACR-2	This study	N/A
ERACR-2 y2 single cut	This study	N/A
ERACR-2 y3 single cut	This study	N/A
e-CHACR-AG	This study	N/A
e-CHACR-AR	This study	N/A
e-CHACR-e	This study	N/A
e-CHACR-k	This study	N/A
Vasa Cas9 resistant to e-CHACR-e	This study	N/A
pAct-Cas9	Gift from Fillip Port	Addgene # 66209
Software and Algorithms		
GraphPad Prism	GraphPad	https://www.graphpad.com/scientificsoftware/prism/
Snapgene	Snapgene	https://www.snapgene.com
Microsoft Excel	Microsoft	N/A

RESOURCE AVAILABILITY

Lead Contact

Further information and requests for resources and reagents should be directed to and will be fulfilled by the Lead Contact, Ethan Bier (ebier@ucsd.edu).

Materials Availability

All unique plasmids or *Drosophila* lines generated by this study are available from the Lead Contact with a completed Materials Transfer Agreement.

Data and Code Availability

Original data have been deposited on Mendeley Data (https://doi.org/10.17632/hjcpd6j8rn.1). Modeling code is available upon request.

EXPERIMENTAL MODEL AND SUBJECT DETAILS

Drosophila rearing and Genetic Experiments

All genetic experiments were conducted in a high-security Arthropod Containment Level 2 (ACL2) barrier facility, in accordance with protocols approved by the Institutional Biosafety Committee from University of California San Diego. All materials and waste are frozen for 48 hours prior to removal from the facility followed by autoclaving. Flies were kept triple-contained in shatter-proof polypropylene plastic vials. Stocks were maintained at 18°C while crosses were carried out at 25°C on a 12 hour day/night cycle on cornmeal media.

Multi-Generational Population cage studies

All population cage experiments were conducted at 25°C with a 12 hour day-night cycle, in 250 mL bottles containing standard cornmeal medium. Seeding populations for all drive experiments included equal numbers of unmated females and males for each genotype. 5-7 days following introduction into the cage and successful mating, all flies (generation n) are removed. Subsequent progeny (generation n+1) were collected, then randomly separated into two pools, one group is further analyzed and screened while the other pool is used for further seeding of the next cage (generation n+2).

METHOD DETAILS

Plasmid Construction

All Constructs were cloned using standard recombinant DNA techniques, including PCR amplification with Q5 Hotstart master mix (NEB #M0494S) and Gibson assembly with NEBuilder HiFi DNA Assembly Master Mix (New England Biolabs, Cat. # E2621).

Please cite this article in press as: Xu et al., Active Genetic Neutralizing Elements for Halting or Deleting Gene Drives, Molecular Cell (2020), https://doi.org/10.1016/j.molcel.2020.09.003

Following successful cloning, the plasmids were transformed into NEB 5-alpha Electrocompetent Competent *E. coli* (New England Biolabs, Cat. # C2989). We list starting plasmids, oligos, and restriction enzymes used to generate each construct. Refer to supplementary materials (Table S2) for full sequences of plasmids and oligos.

MCR-GFP construct by "tagging"

The MCR-GFP construct used for these studies was generated by genetic ''tagging'' of the unmarked prototype yMCR construct (Gantz and Bier, 2015). Briefly, a plasmid construct carrying the eGFP gene expressed under control of the 3XP3 eye promoter, followed by 3′ SV40 polyadenylation sequences, flanked by homology sequences present in the unmarked yMCR construct (*cas9* transgene and U6 gRNA homology arms), and carrying a construct expressing a gRNA directing cleavage between the *cas9* transgene and U6-gRNA of the yMCR was inserted into the genome at the same site as the yMCR using gRNA-y1. Transgenic fly strains carrying this tagging construct (eGFP-Tagger) were recovered and crossed to the yMCR line to generate MCR/eGFP-Tagger females. Single crosses were performed by mating with Basc balancer males and the daughters in the resulting offspring were screened for a y-body color, indicative of Cas9 activity. Vials with Cas9 activity indicated a successful tagging of the yMCR construct and individual males were crossed with cut resistant gRNA-y1 site females (contain static Cas9 at gRNAy1 site) to generate isogenic homozygous stocks for use in this study.

Microinjection of ERACR and e-CHACR Constructs

Plasmids were purified using the QIAGEN Plasmid Midi kit (#12191). ERACR and e-CHACR constructs were co-injected with a transient source of pAct-Cas9 (pAct-Cas9 was a gift from Fillip Port (Addgene plasmid # 62209) by Best Gene Inc. Injection mixes were assembled with either ERACR or e-CHACR donor plasmids (final concentration: 700 ng/μl) and pAct-Cas9 (final concentration: 300 ng/μl) in a volume of 50 μl. ERACR mixes were injected into a w1118 stock (BDSC #5905) while e-CHACR mixes were injected into an Oregon-R stock (BDSC #2376). All constructs were fully sequenced prior to injection and subsequently generated transgenic stocks were confirmed through sanger sequencing as well.

Recovery of Transformants and Genomic DNA Isolation

Injected flies were crossed the w1118 stock and progeny were screened for DsRed or GFP positive individuals, which were then subsequently crossed to an FM7 (first chromosome) or TM3 (third chromosome) balancer. Homozygous lines were established based on the absence of balancer alleles. For analysis of individuals containing gene drive elements, flies were frozen in an ACL-2 facility for 48 hours prior to removal from the facility and DNA isolation. Genomic DNA was prepared from individual male flies according to protocols by Gloor, 1993.

Drosophila PCR and Sequence Analysis

Sequencing PCR reactions were assembled with Q5 Hotstart master mix (NEB #M0494S), KOD Xtreme Hot Start DNA Polymerase (Millipore #71975), Phusion High-Fidelity PCR Master Mix with HF Buffer (Thermo-Fisher #F531S), or Platinum SuperFi DNA Polymerase (ThermoFisher #12351010). Primers used to amplify PCR products are listed in Table S4. PCR samples were purified using the QIAquick PCR purification kit (QIAGEN #28104) prior to sanger sequencing.

QUANTIFICATION AND STATISTICAL ANALYSIS

Mathematical Modeling

Model fitting was carried out for the ERACR-min and ERACR-2 cage experiments using Markov chain Monte Carlo (MCMC) methods in which genotype-specific fitness parameters were estimated, including 95% credible intervals (CrIs). We considered discrete generations and Mendelian inheritance rules at the gene drive locus, with the exception that, for females heterozygous for the ERACR (E) and drive (H) allele, a proportion of the drive alleles are cleaved, while a proportion remain H alleles (Figure S1). Of those that are cleaved, a proportion are subject to accurate homology-directed repair (HDR) and become E alleles, while a proportion become resistant alleles. Of those that become resistant alleles, a proportion become in-frame, cost-free resistant (R) alleles, while the remainder become out-of-frame or otherwise costly resistant (broken, B) alleles. Parameter values were fixed for and based on the experimental results depicted in Figure S12. These considerations allowed us to calculate the expected genotype frequencies in the next generation, and to explore the fitness and assortative mating parameters that maximize the likelihood of the experimental data. Estimated parameters include the fitness cost associated with males having the drive allele, females homozygous for the drive allele, and having one copy of the drive or broken allele in females or respectively. BB females and BY males were known to be unviable. Populations were assumed to be randomly mixing, with the exception of the ERACR-2 experiment, in which females having the y^+ phenotype preferentially mated with males having the y^+ phenotype. For ERACR-2, we estimated an additional parameter representing the fraction by which y^+ females reduce their mating with y^- males. The modeling framework is described in full in the Supporting Information.

Please cite this article in press as: Xu et al., Active Genetic Neutralizing Elements for Halting or Deleting Gene Drives, Molecular Cell (2020), https://doi.org/10.1016/j.molcel.2020.09.003

CellPress

Statistical Methods

Statistical analysis was performed using GraphPad Prism. One-way independent measures ANOVA followed by Sidak's Multiple Comparisons test were performed for graphs in Figures 1D and 6 (all panels). All other graphs use one-way independent measures ANOVA followed by Tukey's post hoc test. Significance was determined as follows: * denotes $p < 0.05$, ** denotes $p < 0.01$, *** denotes $p < 0.001$, and **** denotes $p < 0.0001$.